Numerical Simulation of the Interaction Between Floating Objects and a Gravity Driven Flow

by

Sai Chaitanya Mangavelli

A Thesis Presented in Partial Fulfillment
of the Requirements for the Degree
Master of Science

Approved April 2018 by the
Graduate Supervisory Committee:

Huei-Ping Huang, Chair
Jeonglae Kim
Erica Forzani

ARIZONA STATE UNIVERSITY

May 2018

ABSTRACT

This thesis focuses on studying the interaction between floating objects and an air-water flow system driven by gravity. The system consists of an inclined channel in which a gravity driven two phase flow carries a series of floating solid objects downstream. Numerical simulations of such a system requires the solution of not only the basic Navier-Stokes equation but also dynamic interaction between the solid body and the two-phase flow. In particular, this requires embedding of dynamic mesh within the two-phase flow. A computational fluid dynamics solver, ANSYS fluent, is used to solve this problem. Also, the individual components for these simulations are already available in the solver, few examples exist in which all are combined. A series of simulations are performed by varying the key parameters, including density of floating objects and mass flow rate at the inlet. The motion of the floating objects in those simulations are analyzed to determine the stability of the coupled flow-solid system. The simulations are successfully performed over a broad range of parametric values. The numerical framework developed in this study can potentially be used in applications, especially in assisting the design of similar gravity driven systems for transportation in manufacturing processes. In a small number of the simulations, two kinds of numerically instability are observed. One is characterized by a sudden vertical acceleration of the floating object due to a strong imbalance of the force acting on the body, which occurs when the mass flow of water is weak. The other is characterized by a sudden vertical movement of air-water interface, which occurs when two floating objects become too close together. These new types of numerical instability deserve future studies and clarifications. This study is performed only for a 2-D system. Extension of the numerical framework to a full 3-D setting is recommended as future work.

DEDICATION

I dedicate my work to my parents and friends for their constant support and motivation.

ACKNOWLEDGMENTS

I would like to express my gratitude to Dr.Huei-Ping Huang, my thesis advisor for his constant motivation and support throughout my work. His guidance and advices kept me on track and helped me achieve the objective in an efficient manner.

I would like to thank Dr. Jeonglae Kim and Dr. Erica Forzani for being a part of the thesis committee.

Finally, I would like to thank my friends for supporting me throughout my work and helping in pooling the necessary resources for the research work.

TABLE OF CONTENTS

CHAPTER Page

APPENDIX Page

LIST OF TABLES

LIST OF FIGURES

NOMENCLATURE

A_{cs}	Cross-sectional area(m^2)
L	Length of domain(m)
θ	Angle (degree)
ρ	Density(kg/m^3)
M	Mass of storage tray(kg)
H	Height of domain(m)
c	Speed of sound(m/s)
I_{xx}	Mass Moment of inertia in x-direction($kg.m^2$)
I_{yy}	Mass Moment of inertia in y-direction($kg.m^2$)
I_{zz}	Mass Moment of inertia in z-direction($kg.m^2$)
v	Velocity(m/s)
t	Time(s)
t_{final}	Final Time(s)

Chapter 1

INTRODUCTION

Gravity driven flows utilize the potential of gravity to transport a fluid system. This type of system is gaining importance because of their potential to act as a replacement for the current exhausting technologies that are used in transportation. This provides a need to study the interaction between floating objects and gravity driven flow. In addition, this study will have important practical applications in environmental and renewable fields. Existing studies suggest that different objects interact with the gravity driven flow in different ways based on their physical properties like density, shape, cross-sectional area. These interactions will have an impact on their stability while traversing. The nature of interaction can be quantified based on the rotational and vertical oscillations about its vertical axis.

In order to study the interactions, the system is formulated as a virtual transportation setup where the floating objects are storage trays that need to be transported with minimal oscillatory behavior. In the study, the term storage trays will be used while referring to the floating objects.

Numerical simulation of these interactions has the potential to act as a virtual experimental setup and help in establishing the relationship between the physical parameters, operating conditions and the nature of motion of the storage trays.

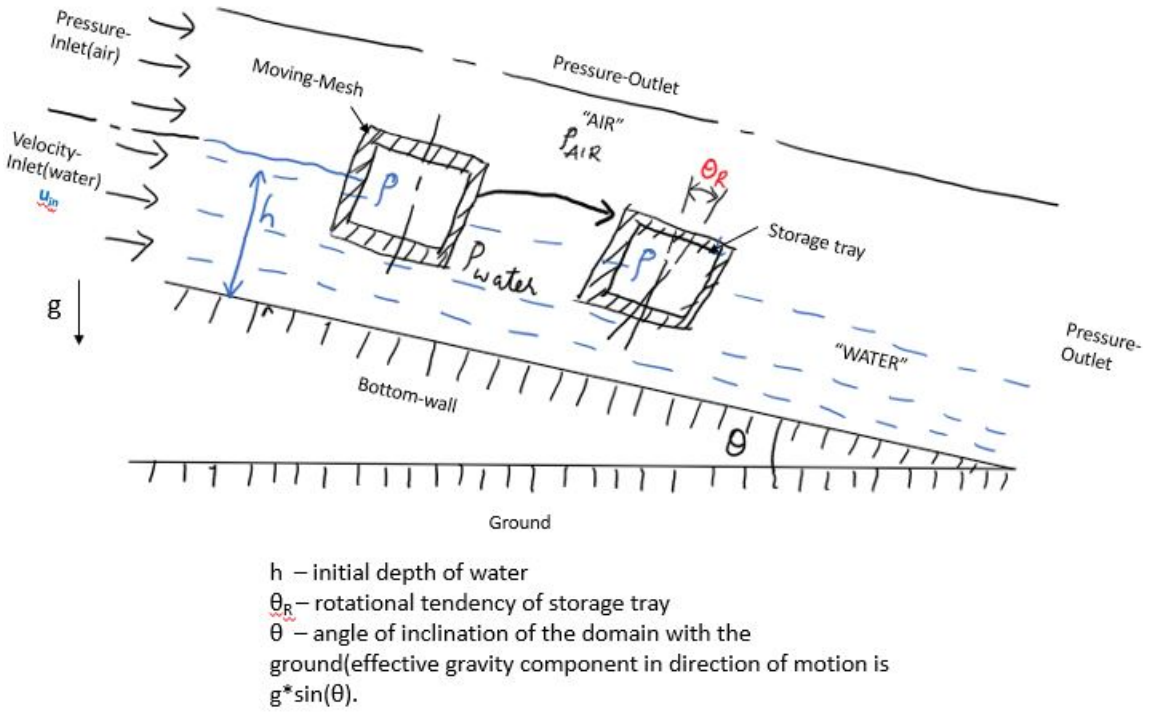

Figure 1: Schematic of the system

The parameters highlighted in blue are the ones varied to understand the interactions. The framework of the setup and numerical simulations developed are generic and can be extended to diversified applications in the same field. The study utilizes a moving mesh setup for a better understanding of the interactions.

1.1 Dynamic Mesh in ANSYS Fluent

ANSYS fluent offers various types of moving mesh settings that enable the user to move the desired object along with a portion of mesh around it. One such setting is dynamic mesh which facilitates motion of a moving object with the following mesh methods (*Dynamic Mesh Update Methods* 2009):

1. Smoothing
2. Layering
3. Remeshing

It also offers the following options:

1. In-Cylinder
2. Six DOF
3. Implicit Update
4. Contact Detection

For simulating a simple linear boundary motion, layering is sufficient. However, for a problem involving rotation and translation like the present study, a combination of smoothing and remeshing will be a better option. In addition, the Six DOF option is used to assign physical properties to the moving mesh to translate and rotate.

1.1.1 Dynamic Mesh Setup

The mesh that is required to move along with the object should be meshed using different elements compared to the rest of the domain. An example is shown below, Quadrilateral mesh is used in the moving region and triangular mesh is used in the rest of the domain.

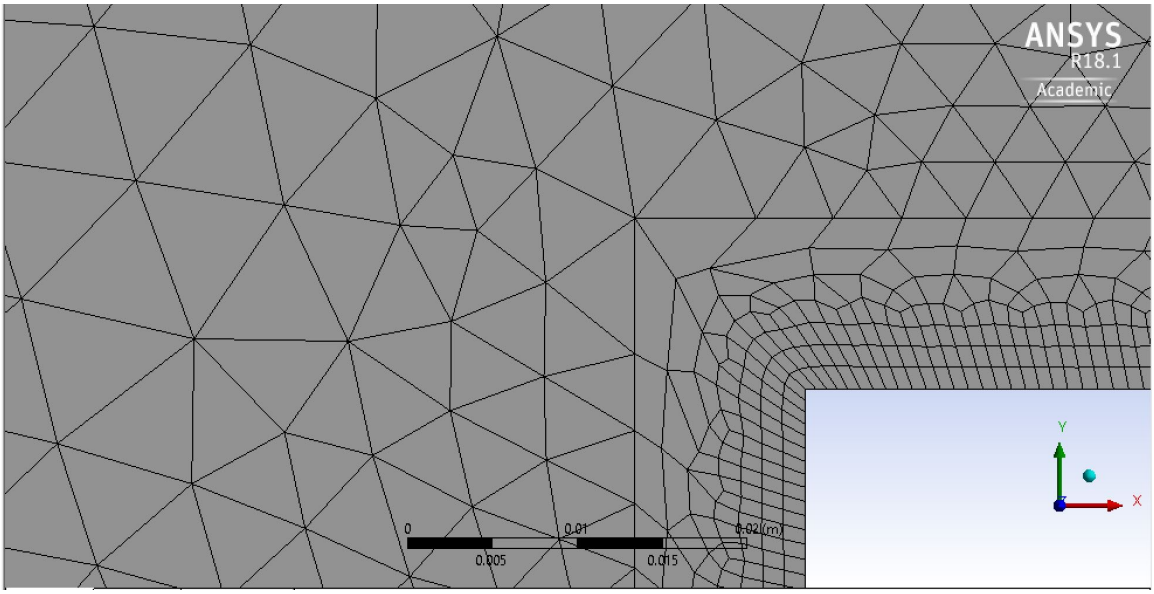

Figure 2: Meshing with different element shapes for dynamic mesh setup

The moving region should be named separately in order to assign properties during the set up of dynamic mesh. The dynamic mesh requires the following inputs:

1. Mesh Scale Information
2. Coordinates of center of mass
3. Initial linear and angular velocity
4. Initial orientation
5. User defined function that provides information about the properties of the fluid, mass and mass moment of inertia of the object.

The detailed setup will be explained in the appendix at the end of the document.

1.2 Literature Survey

The flows that are driven by gravity have been a part of many research studies. They often find applications in chemical coatings, flow of thin films on uneven terrains, interaction of floating objects in suspensions etc.

Gravity is used to drive objects in many applications. The study by Bogner Simon and RüDe, Ulrich reflect the methodology and nature of motion generated. The boundary conditions and nature of surface impact the distribution of fluid momentum. The study further focuses on the forces experienced by the floating objects and their impact on the stability of the object during its motion(Bogner and RüDe 2013).

The angle of inclination of the domain and the density of the object have a significant impact on the equilibrium position of the floating object. The study by Fekken Geert gives an insight on factors affecting the vertical oscillations. The study further demonstrates the impact of the density gradient caused by the multi phase medium on the buoyancy forces responsible for maintaining the equilibrium position (Fekken 2004). This information is utilized in setting up the numerical simulation and selection of the density of storage tray in the current study.

Bogner Simon studied impact of the gravity driven flow on moving rigid bodies in terms of stability analysis based on shape and impact velocity. The research utilized various real world applications while framing the governing equations and other operating parameters during the numerical simulation(Bogner, n.d.)

The VOF method is widely used in numerical simulations of multi phase flows due to its efficient discretization of mass conservation and faster convergence with good results. The study by Vreugdenhil Cornelis Boudewijn gives an insight on

various multi phase models and the corresponding discretization of the conservation laws(Vreugdenhil 2013).

The study by Wörner Martin on implicit model of the VOF and its implications of the error propagation and convergence is utilized in selecting the solver and settings in the current study(Wörner 2012).

Gaskell PH, Jimack PK, Sellier M, Thompson HM and Wilson MCT studied types and nature of equations in multi-phase flow based on applications like shallow water, turbulent flow and sediment flow. This information was useful in understanding the applications of various equations and the assumptions made while using them (Gaskell et al. 2004). Especially the equations and the solver settings used for shallow water cases was informative in setting up the setup for the current study.

Allshouse Michael R, Barad Michael F, Peacock Thomas studied the impact of surface tension of water on the floating object and resulting in propulsion of the block. The study concluded by establishing the theory of the potential of density difference and the angle of attack of water on the non-uniform object in creating a net forward driving force(Allshouse, Barad, and Peacock 2010). This study was very helpful in setting up the initial velocity and depth of water to provide sufficient starting momentum to ensure less rotational tendency.

Zeng K, Pal Deepankar, Gong HJ, Patil Nachiket and Stucker Brent study gave an insight into moving mesh characteristics and equations that govern them(Zeng et al. 2015).

Finally, AMSYS helps section gave an insight on the dynamic mesh setup and various options offered (*Dynamic Mesh Update Methods* 2009).

Despite, lot of research was done in the field, implications of the momentum of water, shape of the object and density of the object on its motion in a gravity driven

flow was not studied. Furthermore, there is no significant research done on the use of dynamic mesh in ANSYS Fluent for the numerical simulation of a gravity driven flow. The current investigation focuses on the study of the above mentioned parameters on the floating objects. Furthermore, it utilizes dynamic mesh setting to track the motion of the object with the help of user-defined functions. The study will also aim at establishing a range of conditions under which the system is numerically stable.

1.3 Problem Statement

1.3.1 Objective

The objective is to study the interaction of the floating object, in this case a storage tray in a medium of water and air that are driven by the gravity. The parameters of interest are rotation and vertical oscillation with respect to vertical axis. A figure depicting the parameters of interest is shown below,

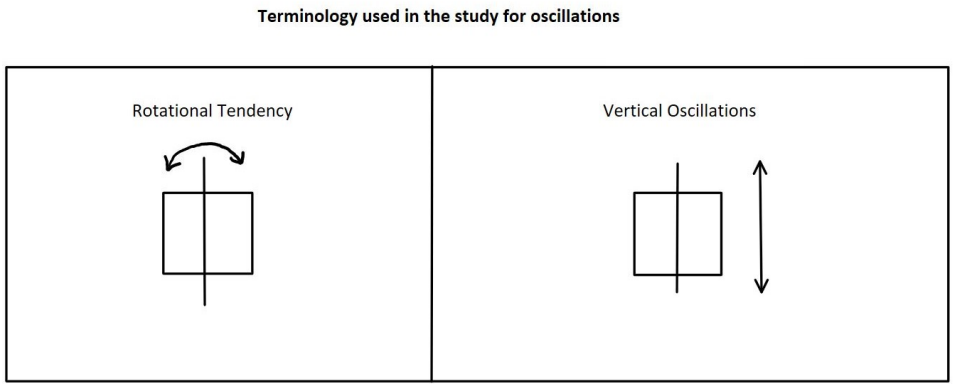

Figure 3: Terminology used in the study for oscillations (numerical stability)- Parameters of Interest

The variables of interest are:

1. Density of the storage tray
2. Shape of the storage tray
3. Spacing between the storage tray (multiple trays)
4. Inlet velocity of water
5. Initial depth of water

1.3.2 General Setup

A rectangular domain encloses the system which is inclined in order to utilize the horizontal component of the gravity to drive the water. A detailed geometry of the general setup with dimensions is depicted below;

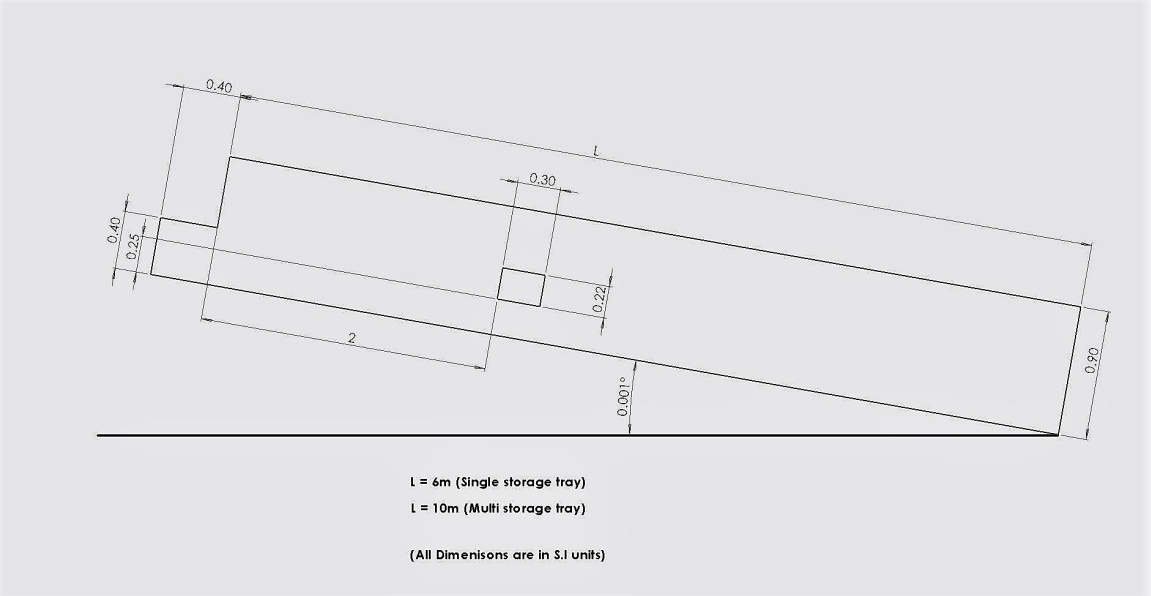

Figure 4: General geometrical setup with dimensions

The length of the domain varies with the number of storage trays to provide sufficient time for tracking the motion of the storage tray. The dimensions and shape of the storage tray are changed as per the required simulation.

The boundary conditions are depicted in the figure below,

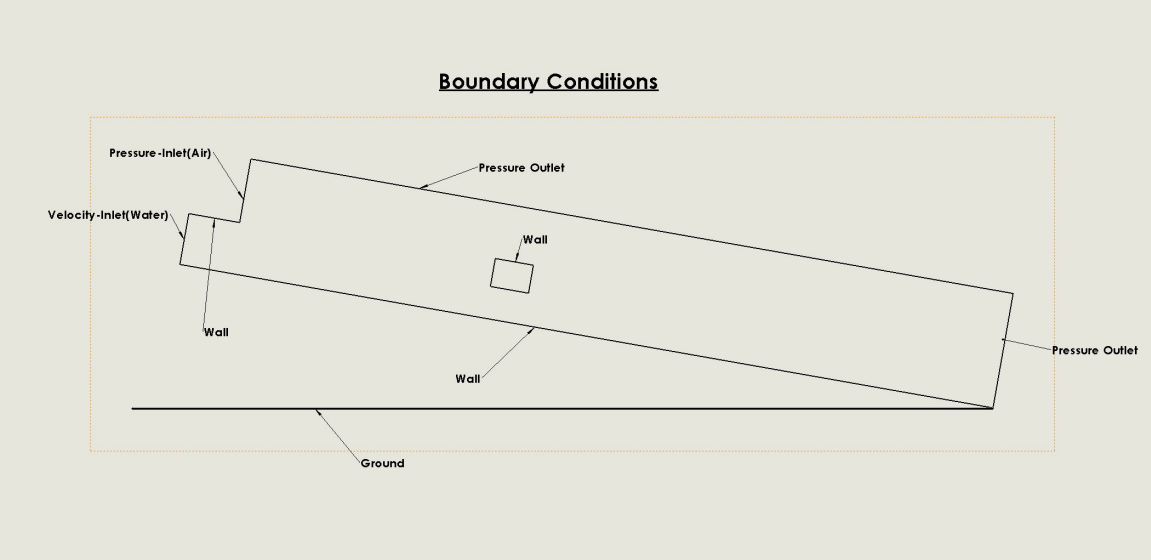

Figure 5: Boundary conditions used in the numerical simulation

An explanation for opting the following conditions is shown in the appendix.

Chapter 2

APPROACH

2.1 Introduction

The study is classified based on the density of block. Within each category, a relation between the rotational and vertical oscillatory behavior and the variables of interest is established.

This chapter will include the storage trays at densities in the range of $500 - 800\,kg/m3$. Rectangular shaped storage trays are used as floating objects with length of domain equal to $6m$. The main aim of the study is to identify the parameter that has maximum influence on the oscillations of the storage tray. Numerical simulations are performed varying all the parameters of interest as discussed earlier and the solutions are obtained from start to the time at which the block reached the outlet.

2.2 Formulation of storage tray in the $\rho = 500 - 800\,kg/m3$

2.2.1 Geometrical Setup

A rectangular domain is used to enclose the system of moving fluid and solid storage tray. A detailed explanation of opting the following dimensions is presented in the appendix. The domain was inclined at an angle to facilitate the action of gravitational force in the direction of motion.

The geometrical setup with the dimensions are shown below,

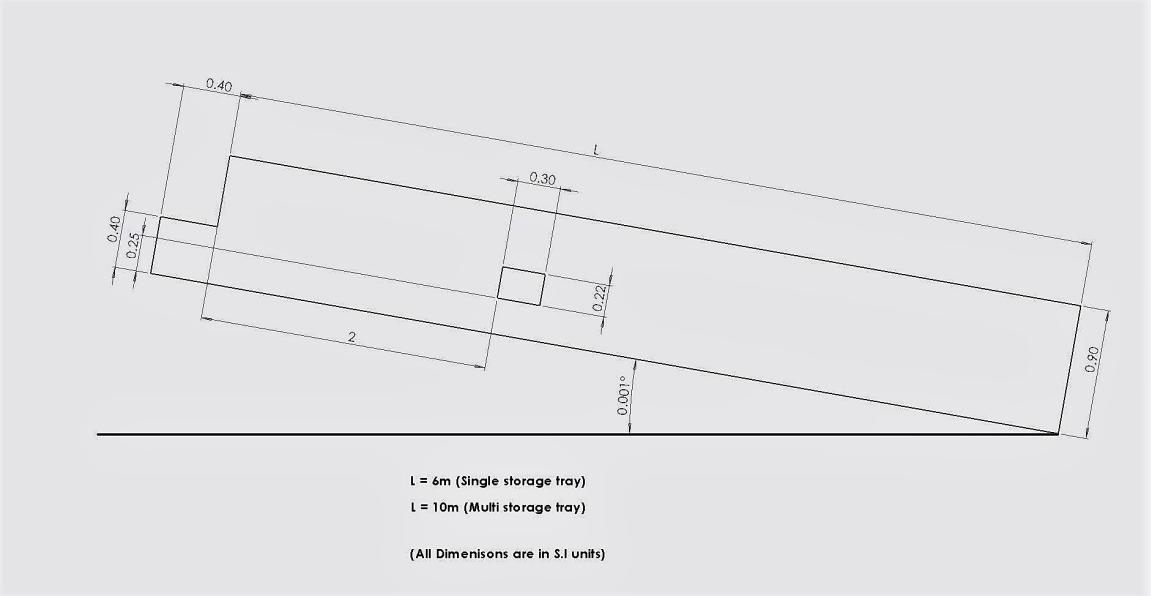

Figure 6: General design of the domain along with storage tray

2.2.2 Mesh Setup

Mesh refinement test is performed to establish a reliable solution. The details of the mesh are shown below,

1. Coarse Mesh: 56676 (number of nodes)
2. Fine Mesh: 128703 (number of nodes)

The result of the rotation of the solid storage tray for both the mesh configurations is graphed below as a part of mesh refinement test,

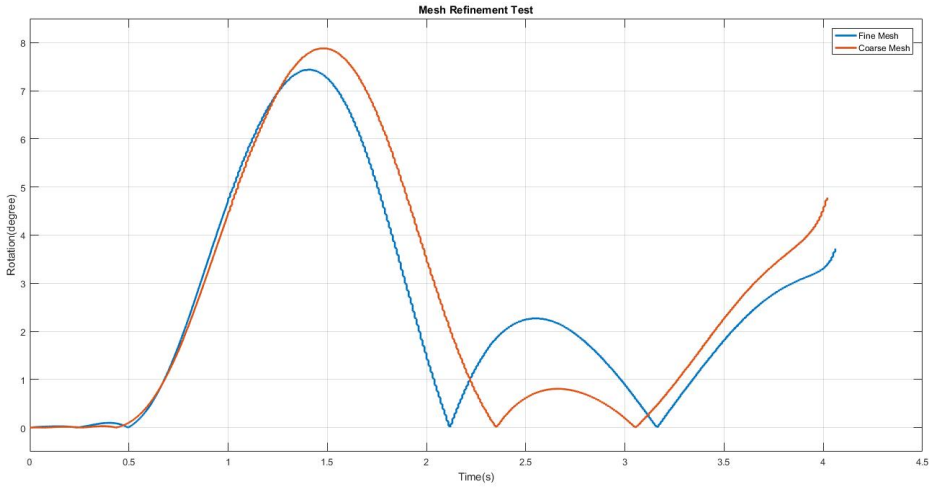

Figure 7: Mesh Refinement Test

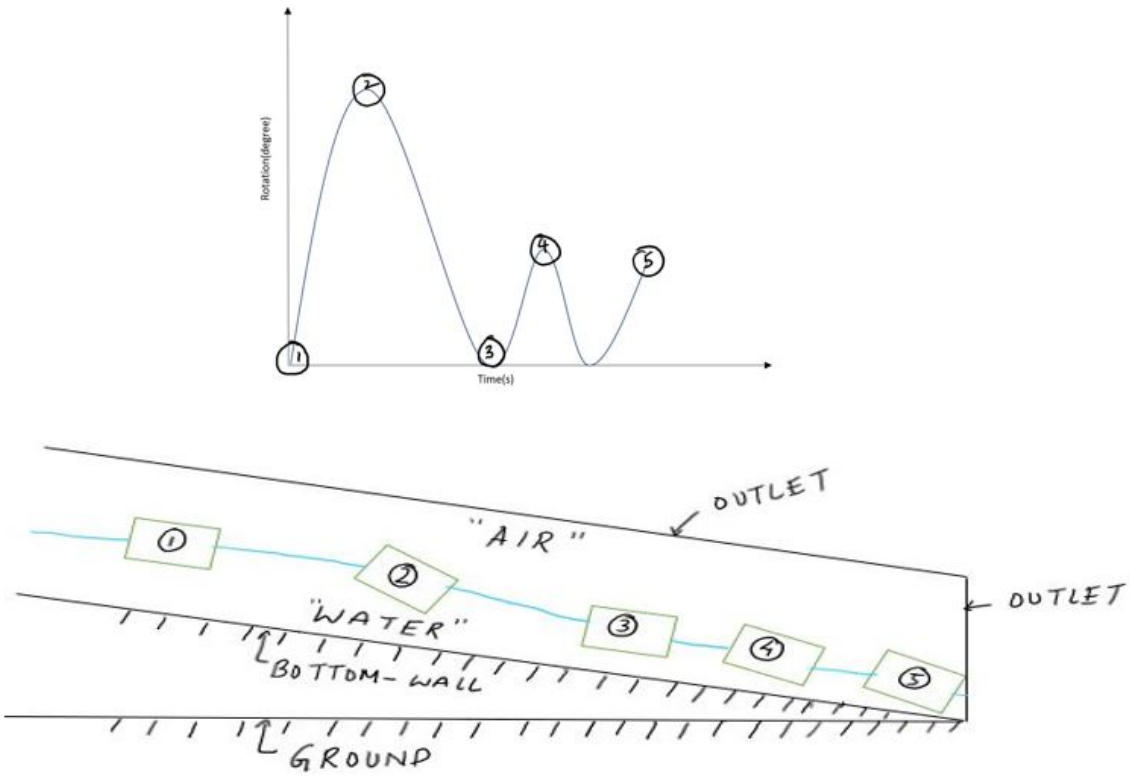

Figure 8: Interpretation of the rotation vs time graph

The fine mesh configuration is shown below,

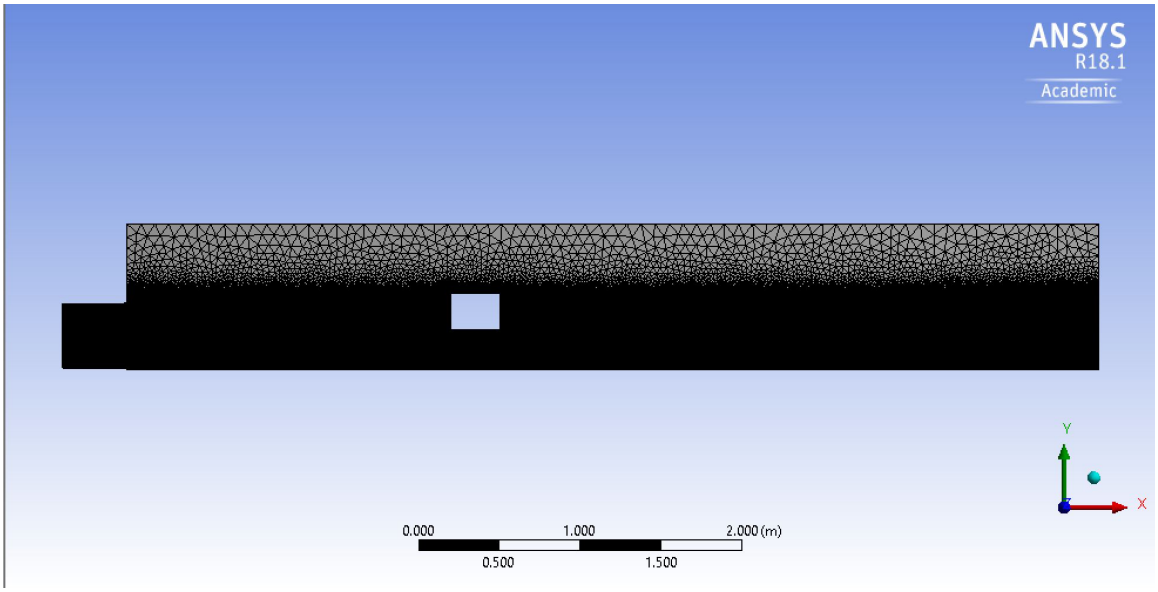

Figure 9: Mesh of the domain with storage tray

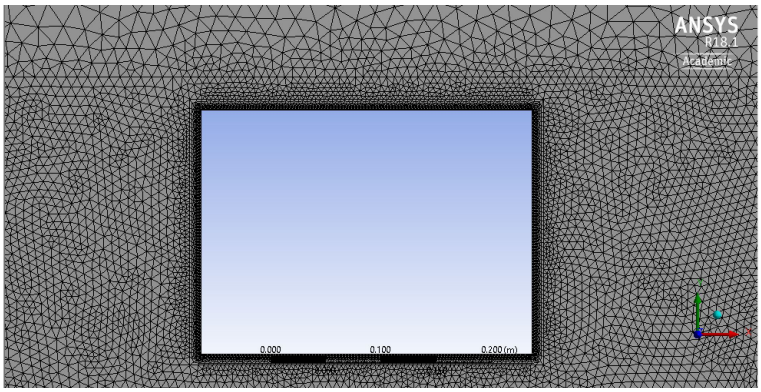

Figure 10: Mesh of the domain with storage tray(zoomed version)

The fine mesh is utilized for all the numerical simulations. It can also be noted that, the mesh is refined near the storage tray. The meshing parameters and statistics for fine mesh are:

1. Number of nodes: 128703

2. Number of elements: 254776
3. Mesh setting: Proximity and curvature with fine setting
4. Face sizing of top half with element size: $0.095m$
5. Face sizing of bottom half with element size: $0.00075m$
6. Refinement: 3
7. Inflation Layers- 20

2.2.3 Simulation

ANSYS fluent module is used to perform the simulations with the following settings:

1. Transient solution with an adaptive time step with initial value of 0.0001.
2. Gravity is turned on
3. Governing equations:
    a) Volume of Fraction with implicit model for Multiphase flow
    b) K-Omega standard model for turbulence
4. Solver settings:
    a) Pressure and velocity coupled
    b) Second order solver for turbulence parameters
    c) PISO solver for pressure

The contour plots are used to inspect both vertical and rotational movement and graphical representation is used to compare the rotational tendency of the storage tray by varying parameters of interest.

2.2.3.1 Analysis with density of storage block as varying parameter

The initial parameters are:

1. Initial Velocity - 0.9 m/s
2. Initial height of water - 0.36 m
3. Pressure inlet for air
4. Pressure outlet for outlet and top surface

The contours of density of mixture are shown below at various times,

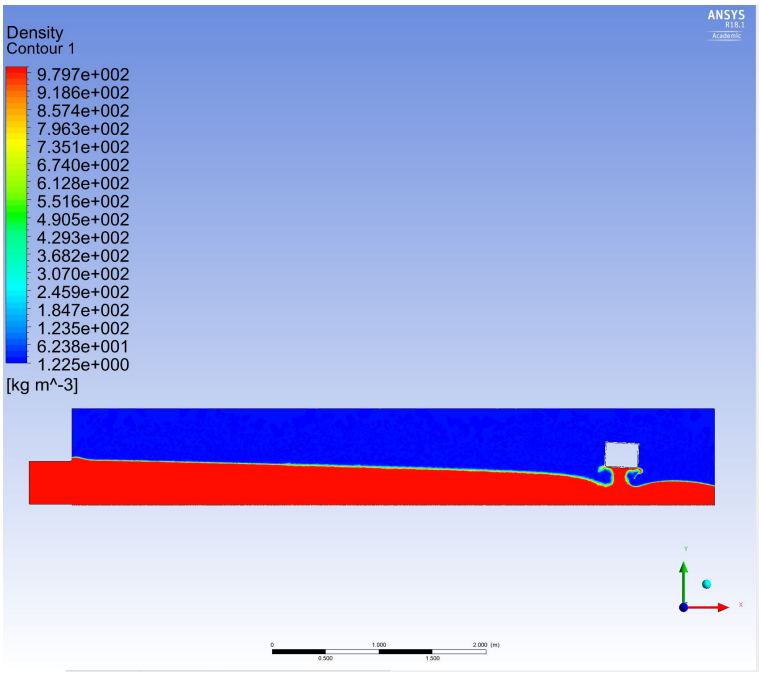

Figure 11: Contour plot of density of mixture at $\rho = 500kg/m^3$ at t=3.87s

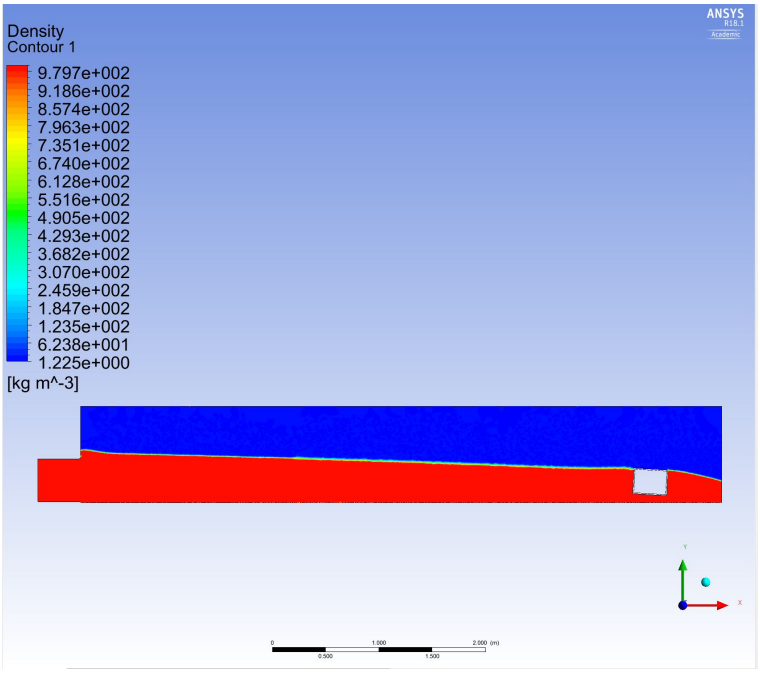

Figure 12: Contour plot of density of mixture at $\rho = 600kg/m^3$ at t=3.7s

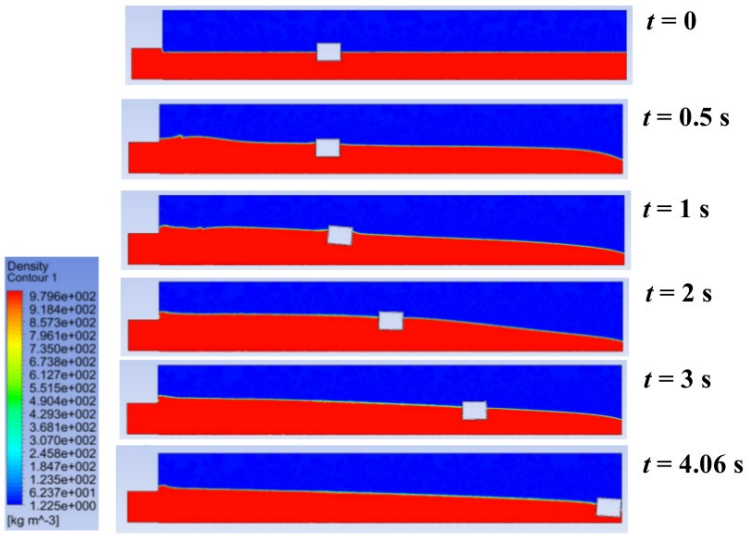

Figure 13: Contour plot of density of mixture at $\rho = 700kg/m^3$

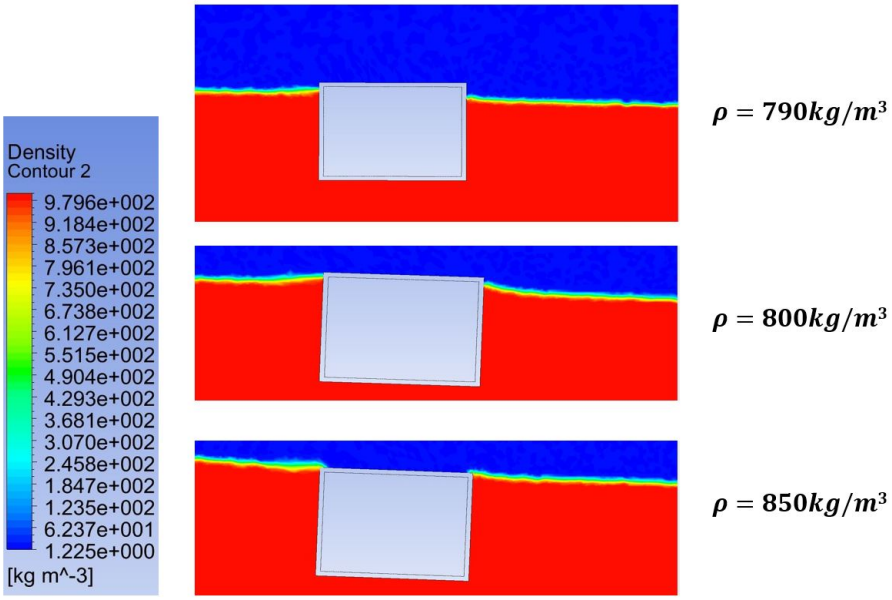

Figure 14: Contour plot of density of mixture at $\rho = 790kg/m^3$, $\rho = 800kg/m^3$ and $\rho = 850kg/m^3$at t=0.5s

From the contour plots, the storage tray becomes numerically unstable at density range of $500 - 600\ kg/m3$ and its vertical oscillations are very high at density range of $800 - 850\ kg/m^3$.

The variation of the rotational tendencies with the density of storage tray is depicted below

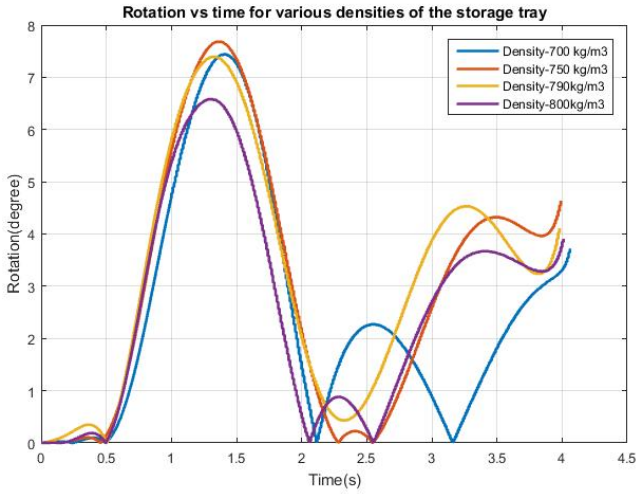

Figure 15: Variation of the rotational tendencies with the density of storage tray

From the graph we can observe that, initially the rotation near $t = 1s$ is slightly increasing with density and then its reducing with density around 800 kg/m^3. This explains the sinking of the block, as the water is reducing the tendency of rotation.

2.2.3.2 Analysis with initial velocity of water as varying parameter

The initial parameters are:

1. Density of storage tray - 700 kg/m^3
2. Initial height of water - 0.36 m
3. Pressure inlet for air
4. Pressure outlet

The contour plots are shown to represent the motion of the storage tray with the

initial velocity of water. The objective of the plots is to establish an understanding of the vertical oscillatory and rotational tendency of the storage tray at the final stage of the motion where higher fluctuations of the storage tray are observed. The contours of density of mixture are shown below. The ones at t=3.8s are only presented as the storage tray was experiencing higher vertical oscillations at that time. Furthermore, since the contour plots of motion of the storage tray are already depicted in the previous section, the rest of the contour plots in the analysis of this section which are similar to the ones in previous section are not shown.

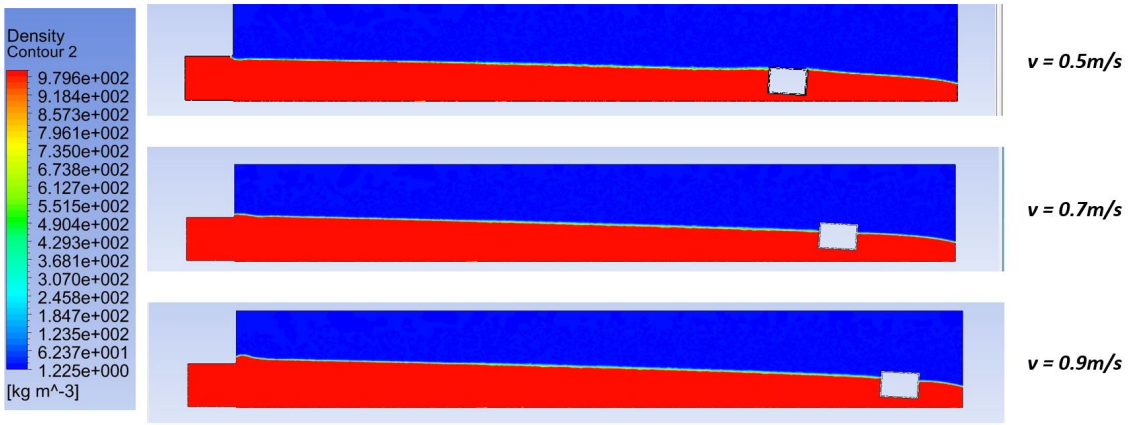

Figure 16: Contour plot of density mixture at v=0.5m/s, v=0.7m/s, v=0.9m/s at $t = 3.8s$

From the contour plots, at lower velocities, due to reduction in momentum of water, the buoyancy force offered by the water is reduced leading to imbalance in the forces in perpendicular direction. Hence, the storage tray's vertical oscillations are very high. The storage tray sinks in water as an effect; leading to numerically instability due to lack of discretization of equations at very low level of water below the storage tray. For the higher velocity cases, the storage tray experiences less vertical oscillations due to equilibrium between the forces and smoothly transitions down the domain.

The variation of the rotational tendencies with the initial velocity of water is depicted below,

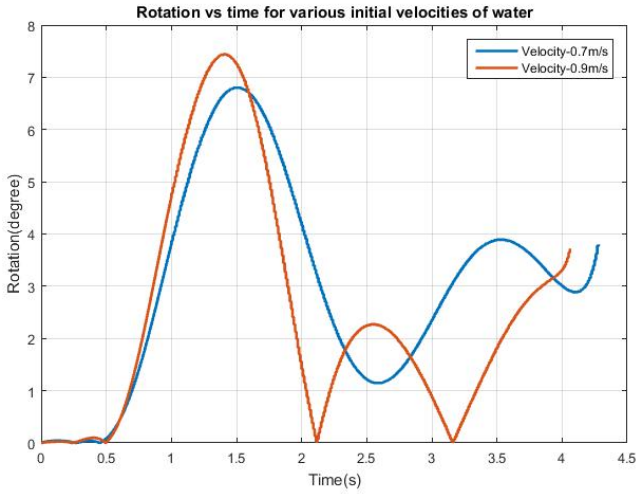

Figure 17: Variation of the rotational tendencies with the initial velocity of water

From the graph we can observe that the low velocity of water facilitates lower initial rotation but leads to a higher rotation as the storage tray moves down the domain. This is expected as the the lower velocity will reduce the force and depth of water the are responsible for the rotation of the storage tray. However, at later stages due to lower levels of water, the dampening of rotation is reduced leading to higher rotational tendency.

2.2.3.3 Analysis with initial depth of water as varying parameter

The initial parameters are:

1. Initial Velocity - 0.9 m/s
2. Density of storage tray - 700 $kg/m3$

3. Pressure inlet for air

4. Pressure outlet

The contour plots of density of mixture with initial depth of water are shown below,

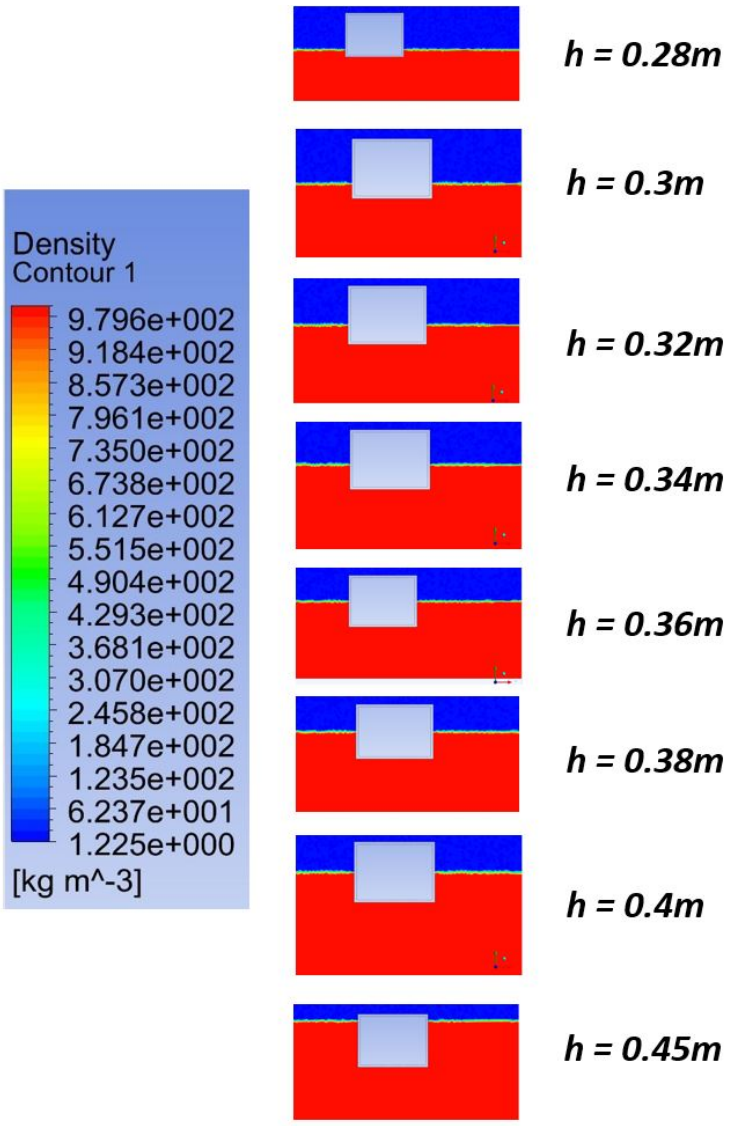

Figure 18: Contour plot of density of mixture with initial depth of water at h=0.28m, h=0.3m, h=0.32m, h=0.34m, h=0.36m, h=0.38m, h=0.4m, h=0.45m at t=0s

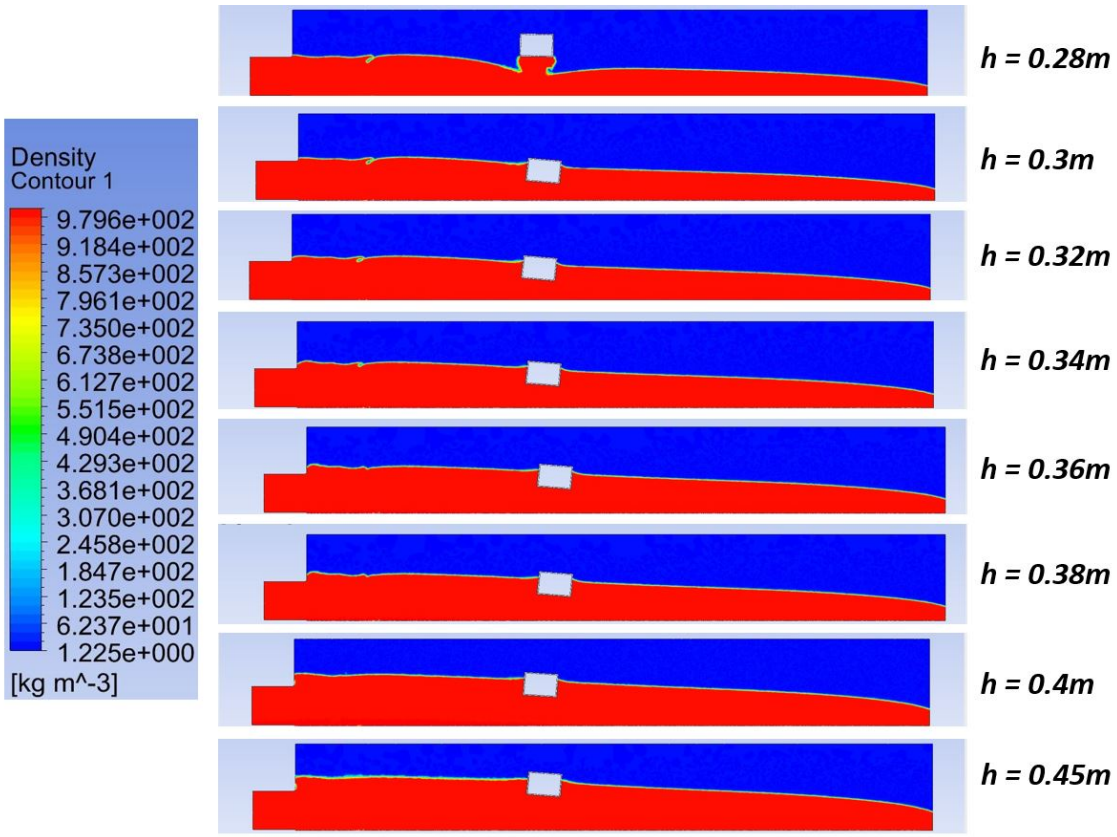

Figure 19: Contour plot of density of mixture with initial depth of water at h=0.28m, h=0.3m, h=0.32m, h=0.34m, h=0.36m, h=0.38m, h=0.4m, h=0.45m at t=1s

At h=0.28m the storage tray experiences high vertical oscillation due to numerical instability as shown by the contour plot at t=1.04s.The vertical oscillations for other values of initial depth of water are dampened.

The variation of the rotational tendencies with the initial depth of water is depicted below,

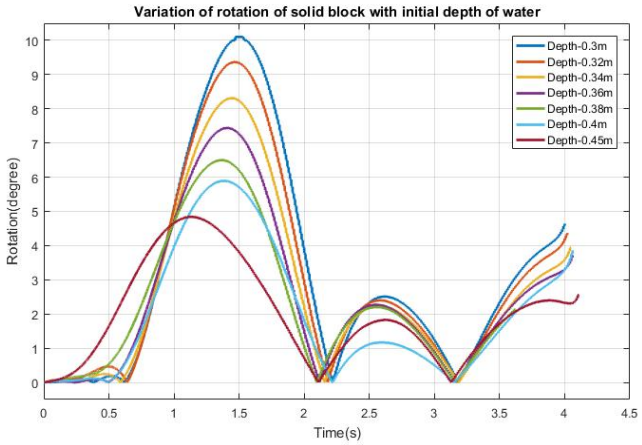

Figure 20: Variation of the rotational tendencies with the initial depth of water

From the graph we can observe that the initial maximum rotation around $t = 1.3s$ due to additional dampening offered by the water. Total flow time is slightly reduced by increasing the water depth. Even at a initial depth of water of $0.45m$ the storage tray adjusts accordingly and stabilizes itself during its motion. However, at a depth of $0.28m$ the block experiences high vertical fluctuations.

2.2.4 Results and Discussion

The simulation contours and plots reflect the range of operating variables within which the numerical simulation can reflect a virtual experimental setup that enables to study the rotational and vertical oscillatory behavior of the storage tray. These range of values are summarized below,

1. Range of storage tray density $= 700 - 800\, kg/m3$

2. Range of inlet velocity of water $= 0.7 - 0.9\, m/s$
3. Range of initial depth of water $= 0.3 - 0.45\, m$

Any condition within this range will lead to a numerically stable system with a smooth transition of the storage tray. However, a system with density of storage tray at $700\, kg/m^3$ with an initial velocity at $0.9\, m/s$ initialized with an initial depth of water at $0.36\, m$ gives the best solution in terms of less rotational and vertical oscillations.

The lift, drag forces and the moment experienced by the storage tray with the best case conditions are graphed below,

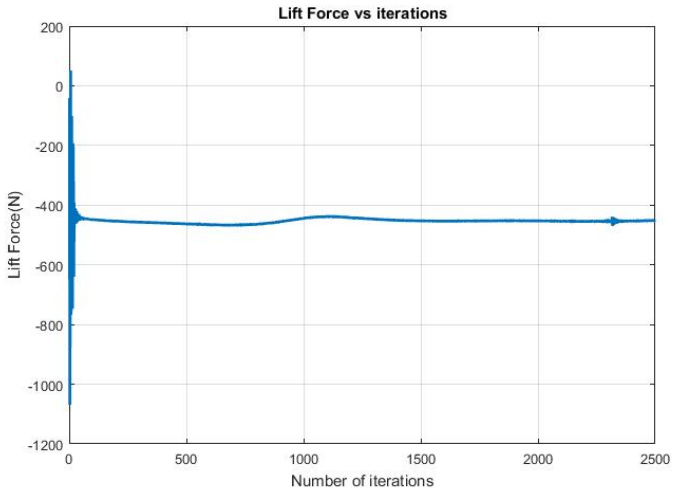

Figure 21: Lift force experienced by the storage tray plotted for the complete flow time

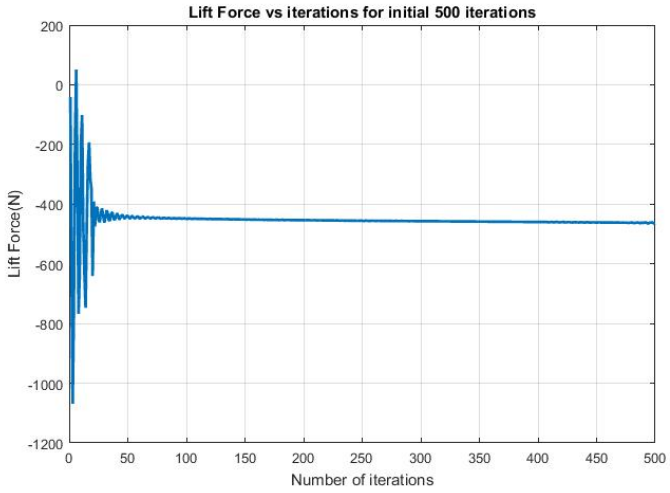

Figure 22: Lift force experienced by the storage tray plotted for the initial part of time

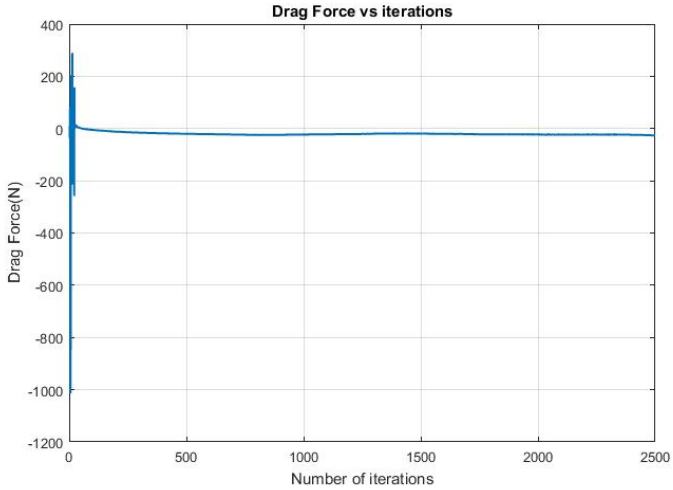

Figure 23: Drag force experienced by the storage tray plotted for the complete flow time

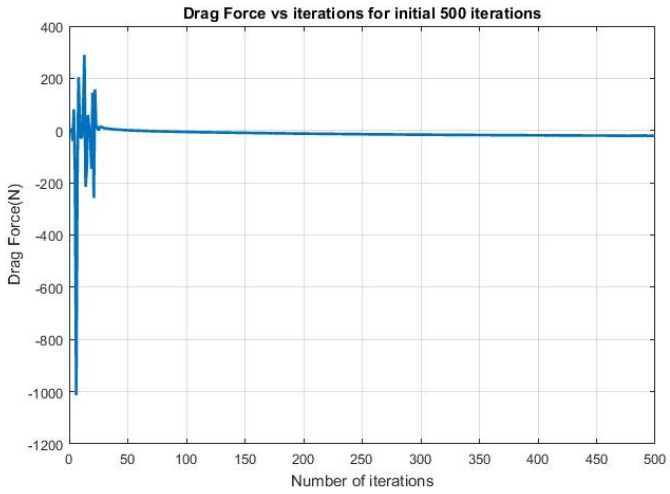

Figure 24: Drag force experienced by the storage tray plotted for the initial part of time

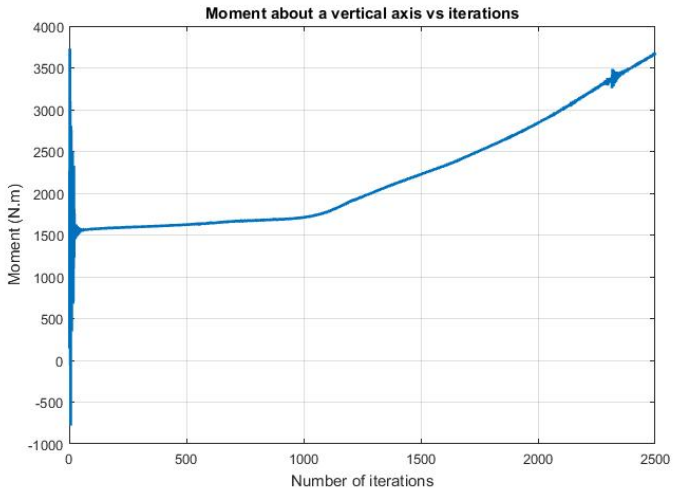

Figure 25: Moment experienced by the storage tray plotted for the complete flow time

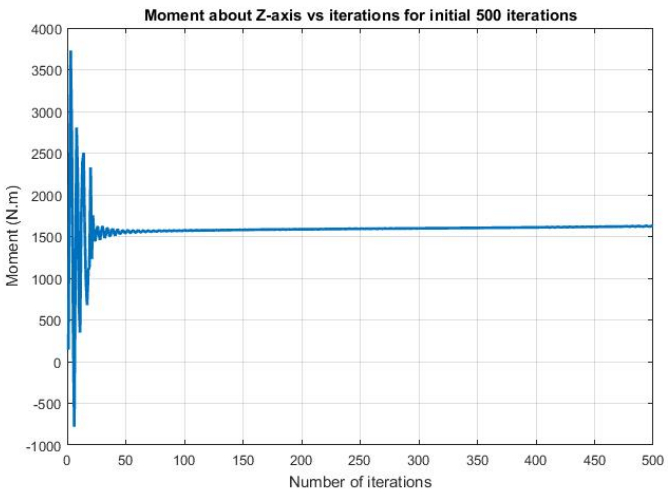

Figure 26: Moment experienced by the storage tray plotted for the initial time

The buoyancy force and the vertical water push due to striking the storage tray at an angle are responsible for the lift force. The momentum gained by water due to its velocity and gravity are responsible for the negative drag force that is reflected in the graph. The moment is the rotating tendency created by the combination of these forces. The slope of the domain is maintained very low so that the acceleration in the direction of motion is just sufficient enough to move the storage tray against the resistance offered by water. The graphs reflect an initial fluctuation in the values of lift,drag forces and moment until flow time of $1s$. After the initial phase, the forces attain a steady value. The moment however has an increasing trend due to the slight sloping of water due to gravity and change in the forces due to change in water level. This is the reason why the storage tray tends to rotate more as it approaches the outlet. For the cases that are out of the operating range, due to imbalance in the forces, the storage tray sinks and this reduces the level of water between the bottom surfaces of the storage tray and the domain. This induces a numerical instability into the simulation that results in the abnormal behavior. So, in these cases, the

numerical simulation fails to represent the real life system. That is why the term numerical instability is used. The only exception to this case, is the system with density of storage tray at 850 kg/m^3 where the numerical simulation has the potential to represent the real system analysis as the storage tray successfully travels down the domain. However, this case is categorized in the fail category due to its high vertical oscillations near the outlet leading to momentary sinking of the block.

2.3 Formulation of Storage tray at high density

2.3.1 Introduction

From the previous section, the solid storage tray at higher densities are initially less stable in terms of vertical oscillations. So, in order to stabilize the storage tray, non-uniform shaped designs are implemented. Since the properties of the storage tray are given using mass and moment of inertia, the net cross-sectional area of the storage tray is reduced maintaining the same density. This will act as a storage tray with non-uniform density for the simulation purposes. In addition, this study will help establish a relation between shape of the storage tray and its oscillatory behavior.

The study is classified into two parts namely type-1 and type-2. In type-1, the design is a rectangular shaped non-uniform storage tray and in type-2, the design is a trapezoidal shaped storage tray. A maximum of 35% reduction in cross-sectional area was employed.

The properties for rectangular and trapezoidal shaped non-uniform storage trays used in UDF are calculated as shown;

1. $M = \rho * A_{cs}$

2. I_{xx}, I_{yy}, I_{zz} are derived from the "Mass Evaluate Section" of the SOLIDWORKS design

I_{xx}, I_{yy}, I_{zz} are mass moment of inertia of the storage trays.

Since it was a 2-D analysis, I_{zz} was sufficient to run the numerical simulations as per dynamic mesh requirements. The initial depth of water varies as the center of mass of the storage tray varies with cross-sectional area. The initial velocity is set at 0.9 $/s$ and density of the storage tray is 850 $kg/m3$. Since solid storage tray just started sinking in the rage of $\rho = 800 - 850\ kg/m3$, the higher end density is chosen.

2.3.2 Analysis of Type-1 design

2.3.3 Geometrical Setup

The geometrical design with dimensions is shown below,

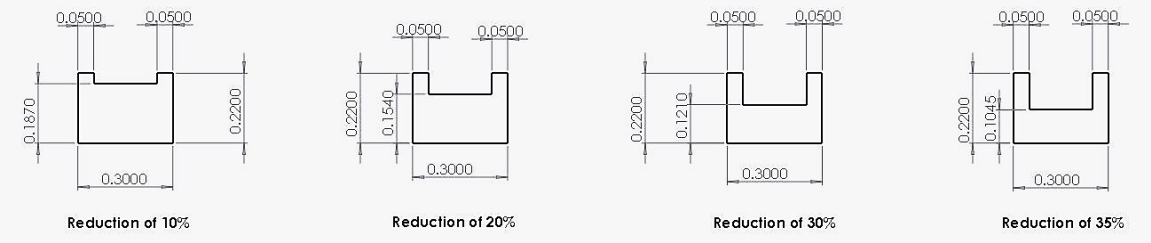

Figure 27: Geometrical design of the type-1 design with reduction in cross-sectional area

2.3.3.1 Analysis with reduction in cross-sectional area as varying parameter

The contour plots of the density of mixture with varying cross-sectional area at

1. t = $0s$
2. t = $1s$
3. t = t_{final}

where higher rotational and vertical oscillations are observed are shown below,

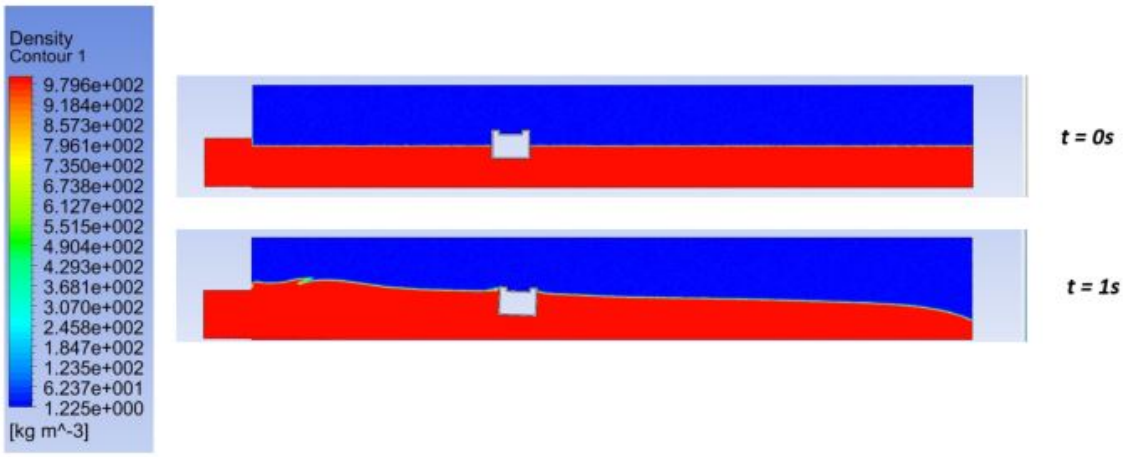

Figure 28: Contour plot of density of mixture with 10% reduction in cross-sectional area

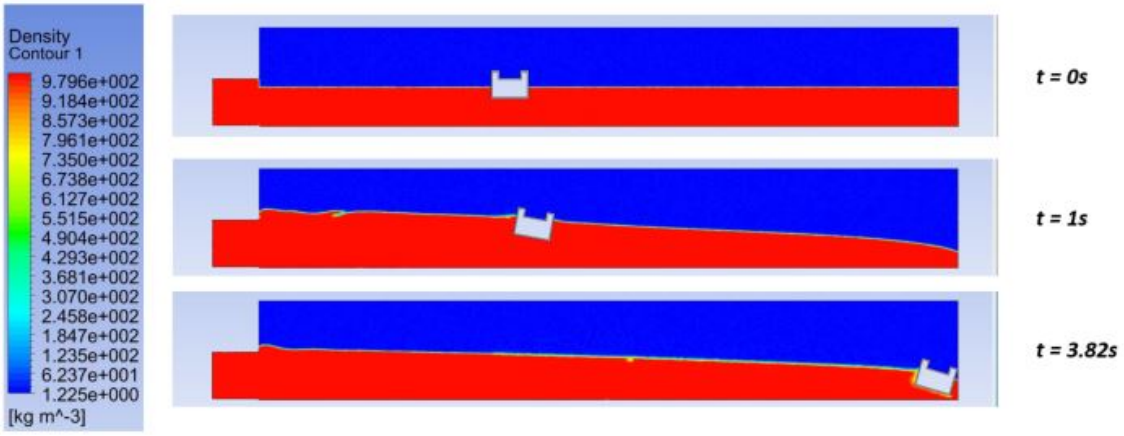

Figure 29: Contour plot of density of mixture with 20% reduction in cross-sectional area

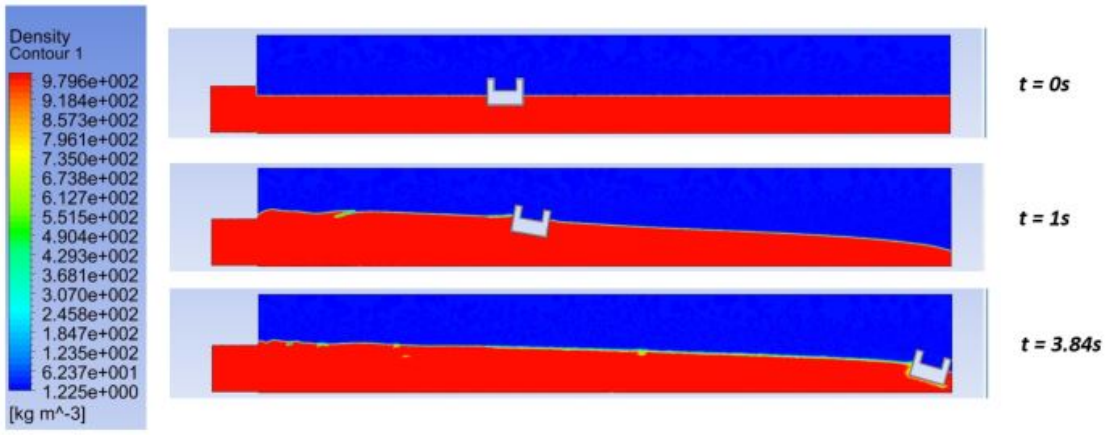

Figure 30: Contour plot of density of mixture with 30% reduction in cross-sectional area

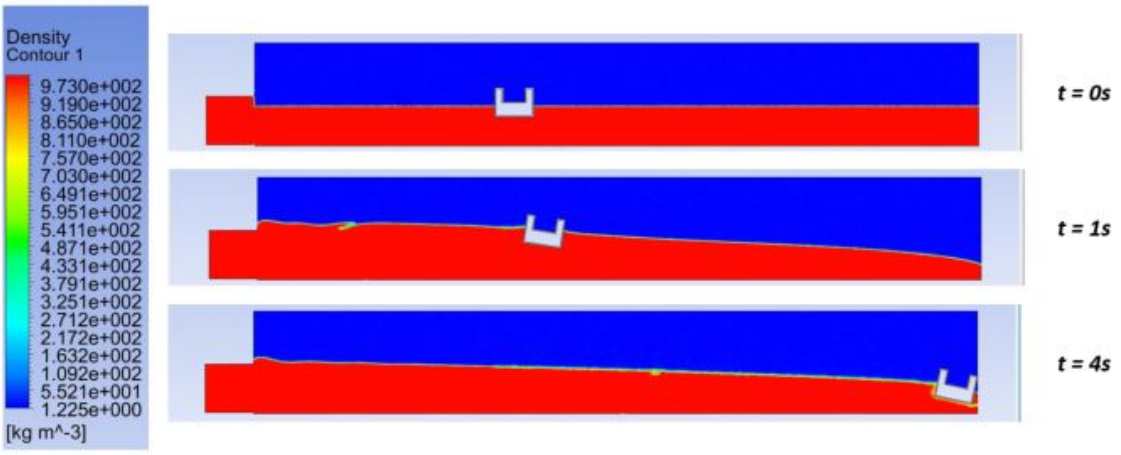

Figure 31: Contour plot of density of mixture with 35% reduction in cross-sectional area

The rotational tendency of the type-1 designs are graphed below,

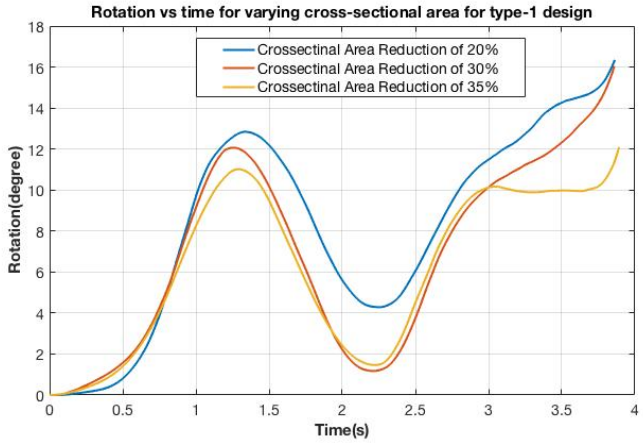

Figure 32: Rotational tendency with varying cross-sectional area for type-1 design

2.3.4 Analysis of Type-2 design

2.3.5 Geometrical Setup

The geometrical design is shown below,

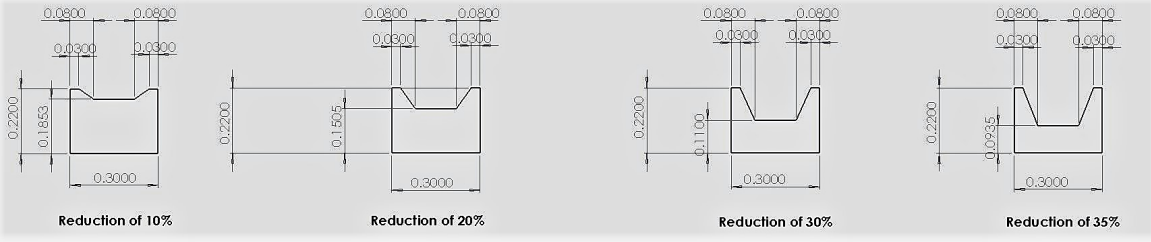

Figure 33: Geometrical design of the type-2 design with reduction in cross-sectional area

2.3.5.1 Analysis with reduction in cross-sectional area as varying parameter

The contour plots of the density mixture at times where high oscillations are observed are shown below,

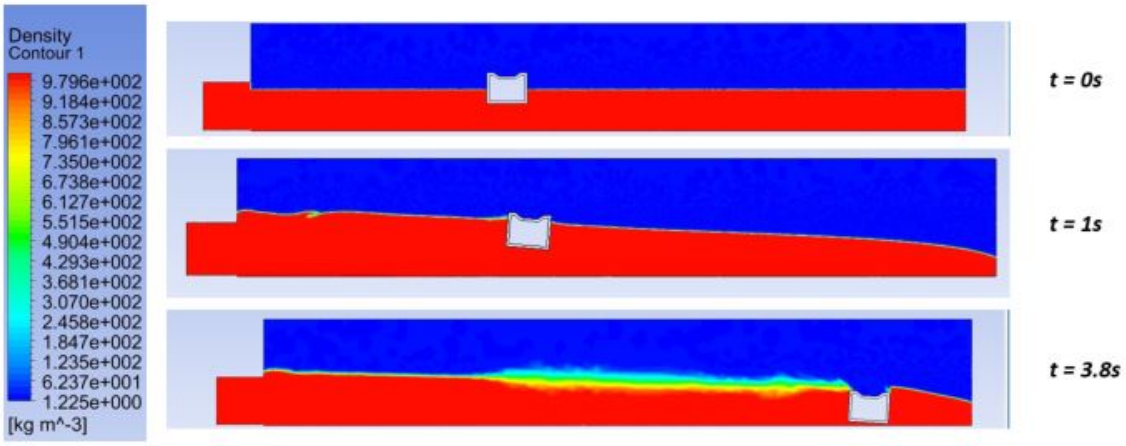

Figure 34: Contour plot of density of mixture with 10% reduction in cross-sectional area

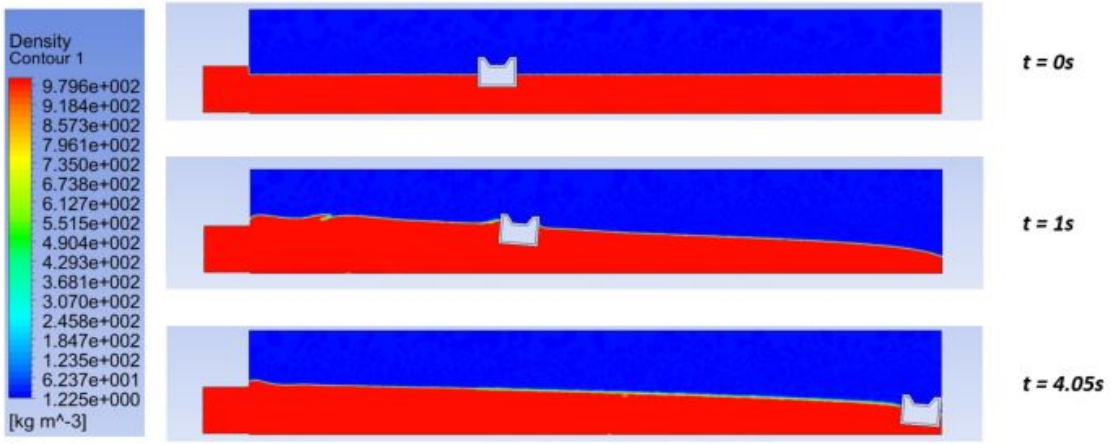

Figure 35: Contour plot of density of mixture with 20% reduction in cross-sectional area

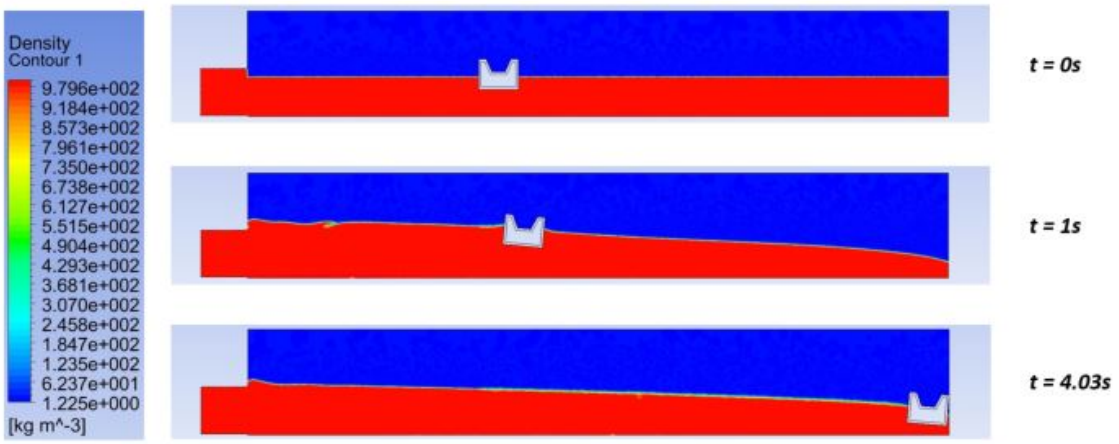

Figure 36: Contour plot of density of mixture with 30% reduction in cross-sectional area

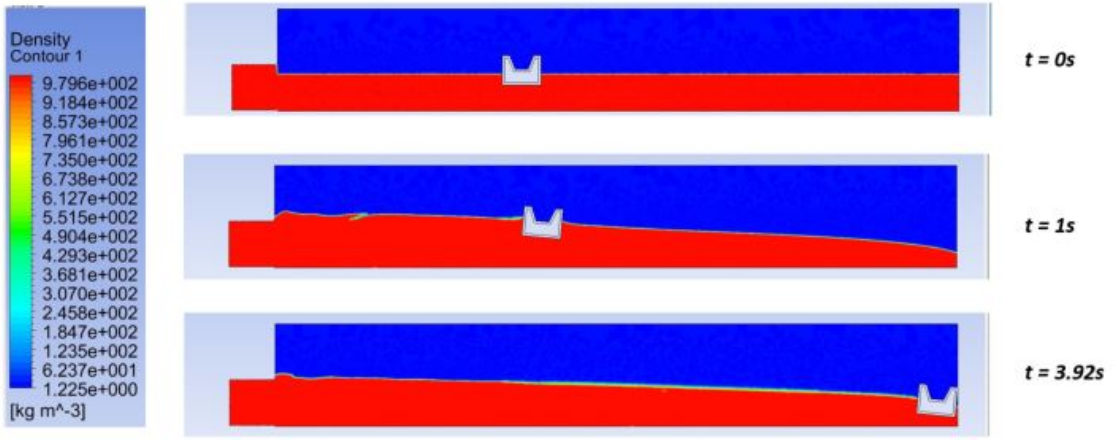

Figure 37: Contour plot of density of mixture with 35% reduction in cross-sectional area

The rotational tendency of type-2 designs are graphed below,

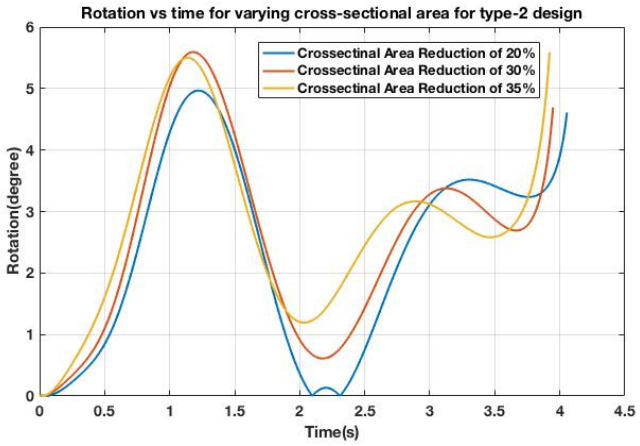

Figure 38: Rotational tendency with varying cross-sectional area for type-1 design

2.3.6 Results and Discussion

The storage tray at 10% reduction in cross-sectional area experiences high vertical oscillations at $t = 1s$ and $t = 3.8s$ for both types of designs as reflected by the contour plots. A further reduction in the cross-sectional area facilitates the dampening of the vertical oscillations and achieves the objective of the section. The reduction in cross-sectional area stabilizes the vertical oscillations and prevents the storage tray from sinking at higher density.

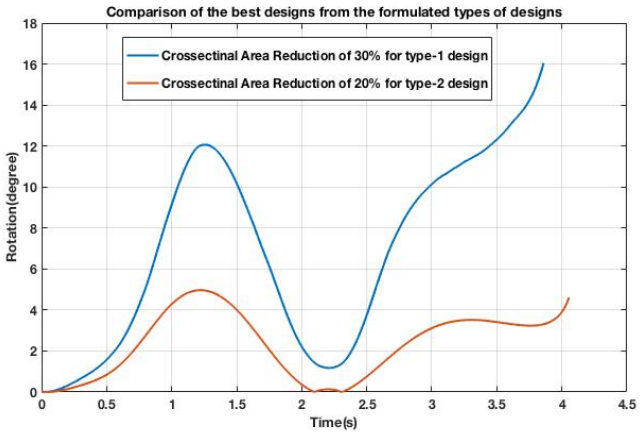

Figure 39: Rotational tendency comparison for two proposed designs

From the above graph, the rotational and vertical oscillations experienced by the type-2 design i.e., the trapezoidal shaped hollow storage tray is relatively less compared to the type-1 design. Hence, the type-2 designs are opted as a preferable one. Even, in the type-2 design, the storage tray with 20% reduction in cross-sectional area is relatively more stable compared to other ones.

The storage trays with non-uniform density show a higher rotational and vertical oscillatory tendency. The quantification of this is shown in the graph below plotted between the best case of hollow tray which is the type-2 case with 20% reduction in cross-sectional area and solid storage tray at $\rho = 700kg/m^3, \rho = 850kg/m^3$, $v = 0.9m/s$, $h = h_{cg}$.

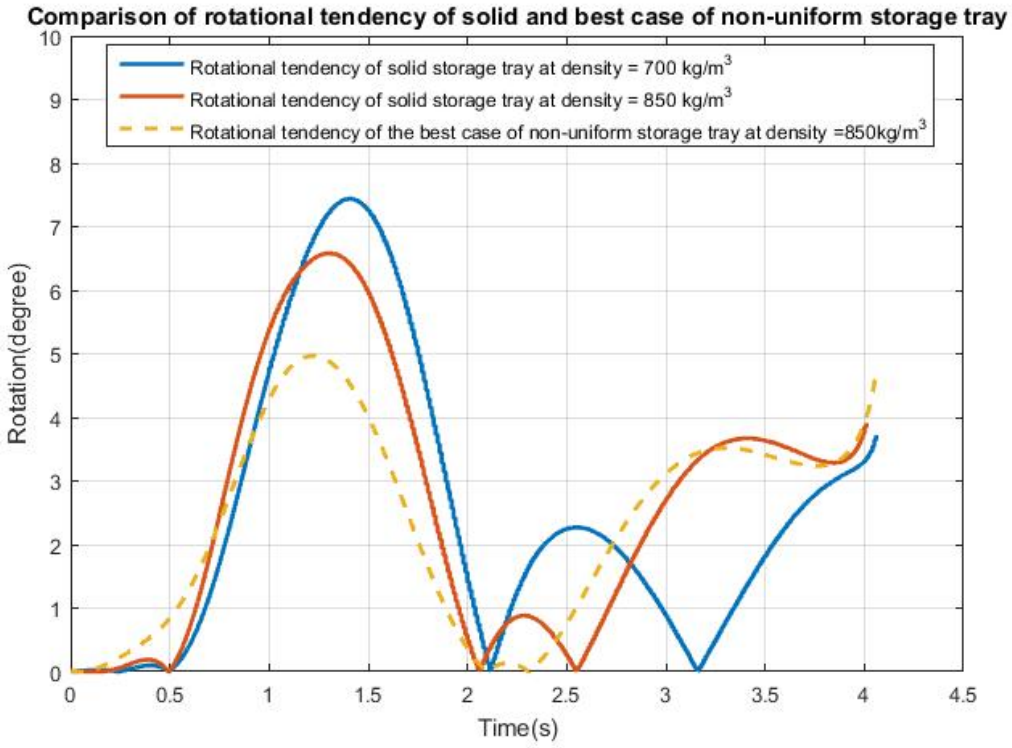

Figure 40: Comparison of rotational tendency among solid and storage trays with non-uniform density

The lift, drag forces and moment for the best case condition are graphed below,

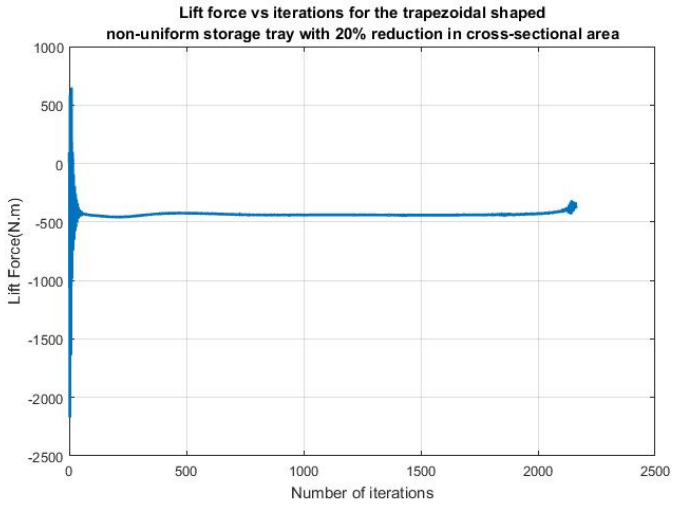

Figure 41: Plot of lift force for type-2 design with trapezoidal shaped storage tray with non-uniform density with 20% reduction in cross-sectional area

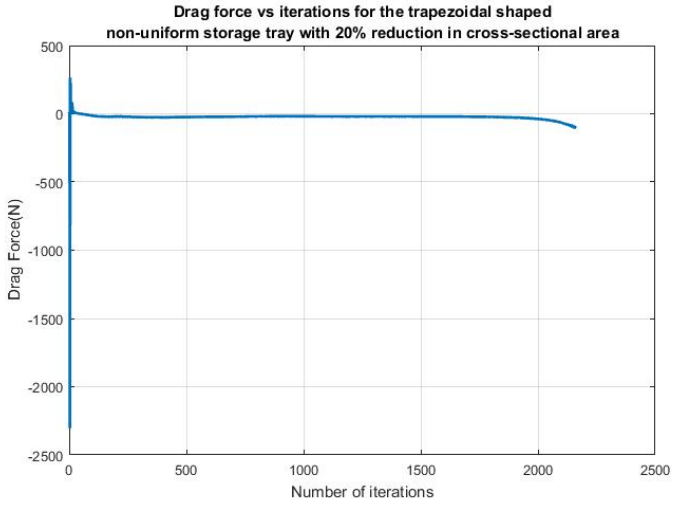

Figure 42: Plot of drag force for type-2 design with trapezoidal shaped storage tray with non-uniform density with 20% reduction in cross-sectional area

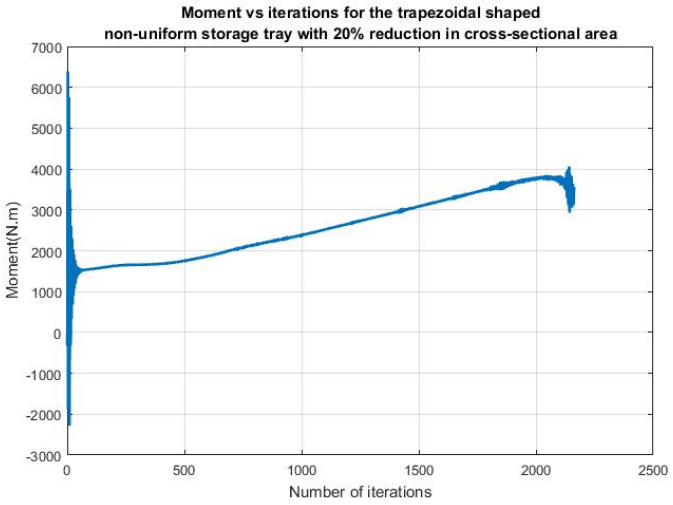

Figure 43: Plot of moment for type-2 design with trapezoidal shaped storage tray with non-uniform density with 20% reduction in cross-sectional area

Similar to the solid storage tray, the forces and moments initially oscillate till the vertical stability is restored. Then the steady value of lift force maintains the vertical stability. The lift force however, experiences slight oscillations at the final stage to unlike solid storage tray case. This is the reason why even the moment is fluctuating at the final stages. These are responsible for a slightly higher rotational tendency for the non-uniform storage tray compared to solid storage tray. The steady value of drag force is negative indicating a driving force in the direction of motion.

2.4 Formulation of multiple storage trays

2.4.1 Introduction

From the previous sections, the best possible setup established for a single storage tray case is used to simulate the multiple storage trays. The objective is to study the extension of the stable conditions of a single storage tray to multiple storage trays

and establish a relation of its motion with spacing between them. The relative change in spacing was monitored to quantify the effect of the accelerated flow due to gravity on the motion of multiple storage trays.

The minimum number of storage trays used are three and the maximum are four. The reason for opting three storage trays instead of two is to observe the impact of the diversified movement of the first and third storage trays on second one in terms of its oscillatory behavior. In addition to that, the stable setup of the three storage trays can be generalized to the case with two storage trays.

2.4.2 Analysis of 3 storage trays with initial spacing as varying parameter

2.4.3 Geometrical Setup

The domain is increased to $10m$ to sufficiently monitor the motion of all storage trays. All the other conditions are maintained similar to the single storage tray case. The geometrical setup of the 3 storage trays is shown below,

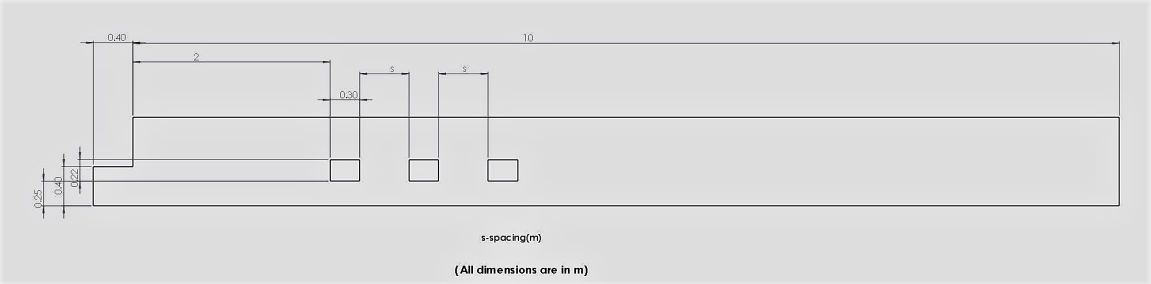

Figure 44: Geometrical setup of the system with 3 storage blocks

An initial spacing of $0.3m, 0.4m, 0.5m, 1m$ are used.

The contour plots of density of mixture as a function of initial spacing are shown below at times where a higher rotational and vertical oscillatory behavior is observed,

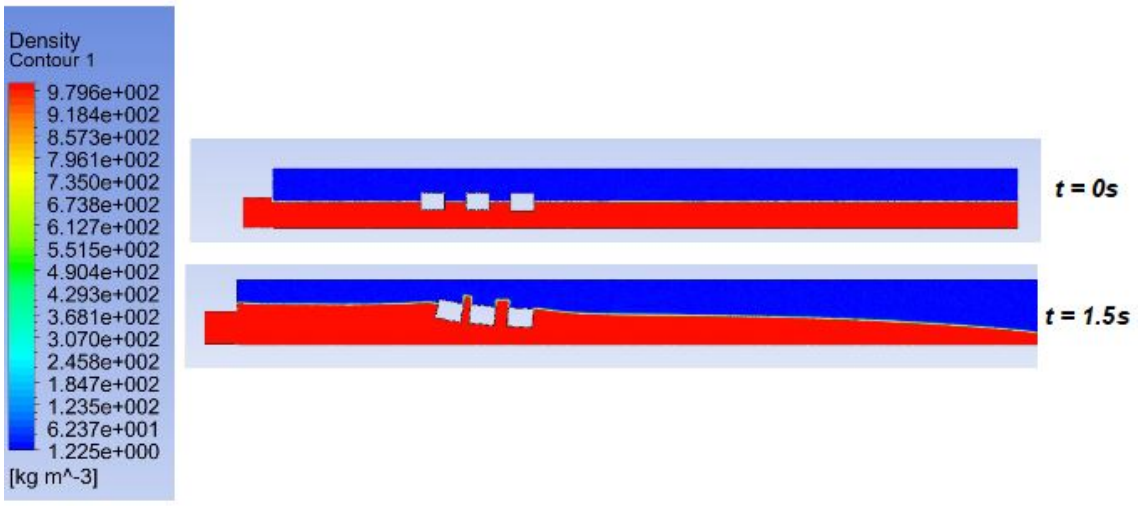

Figure 45: Contour plot of density of mixture with initial spacing of $0.3m$

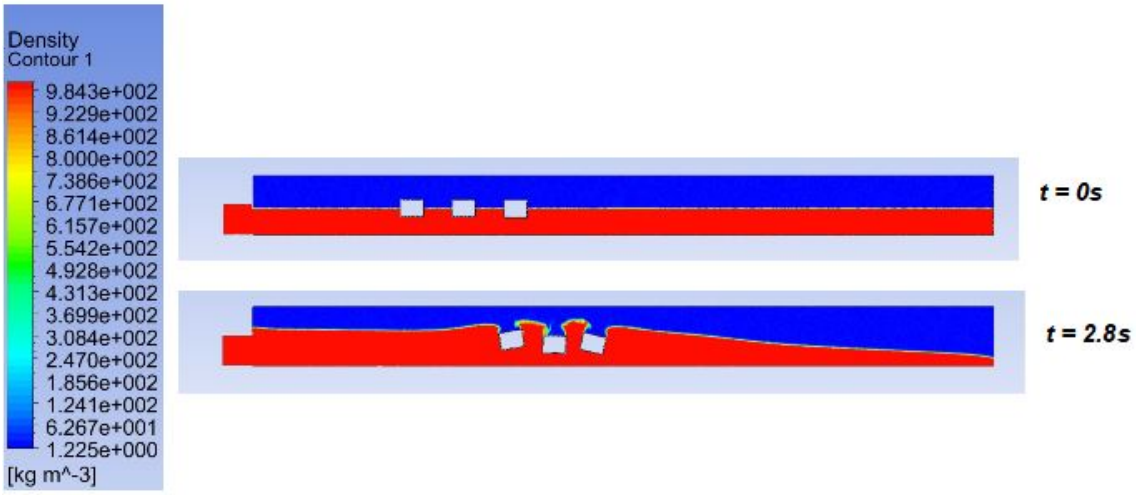

Figure 46: Contour plot of density of mixture with initial spacing of $0.4m$

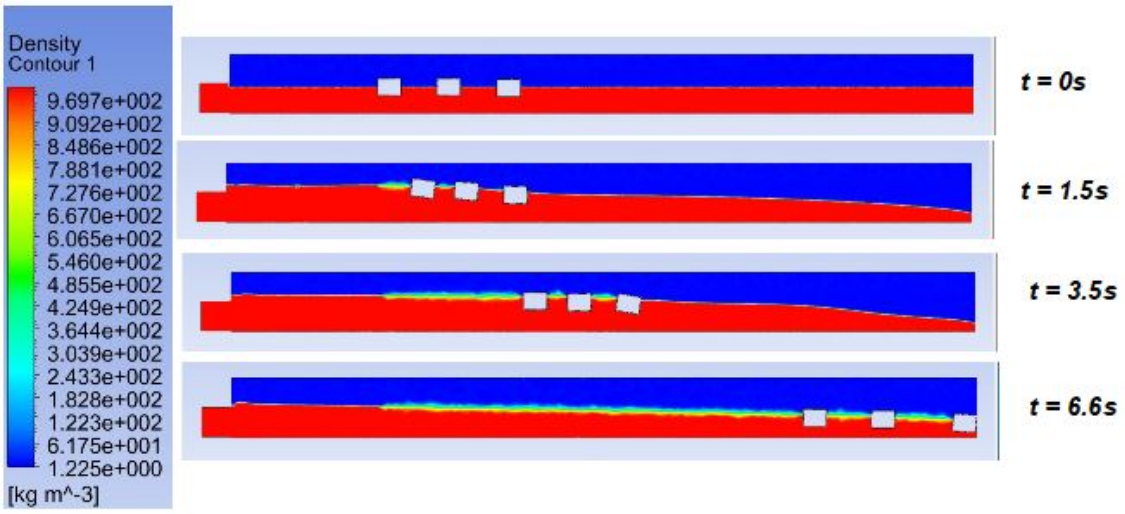

Figure 47: Contour plot of density of mixture with initial spacing of $0.5m$

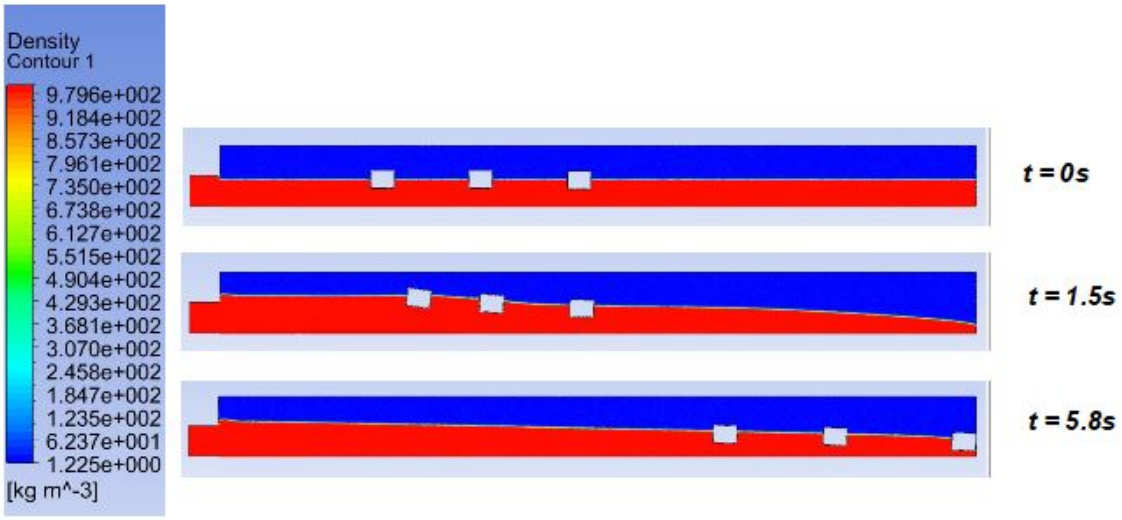

Figure 48: Contour plot of density of mixture with initial spacing of $1m$

2.4.3.1 Results and Discussion

The contour plots reflect the sensitivity of the motion with initial spacing. The system with a spacing of $0.3m$ and $0.4m$ lead to numerical instability due to high vertical oscillations. The initial distribution of momentum of water lowering the driving

force on storage trays along with inertial effect lead to a slow horizontal movement. In addition failure of restoring a balance between buoyancy and gravitational force at initial times lead to high vertical oscillations. This explains the numerical instability of the storage trays at lower spacing.

The results at higher spacing of $0.5m$ and $1m$ show a stable transition of the storage trays. So, a minimum spacing of $0.5m$ is required to numerically simulate the storage trays motion. The rotational tendencies of the three storage trays at the above spacing is graphed below,

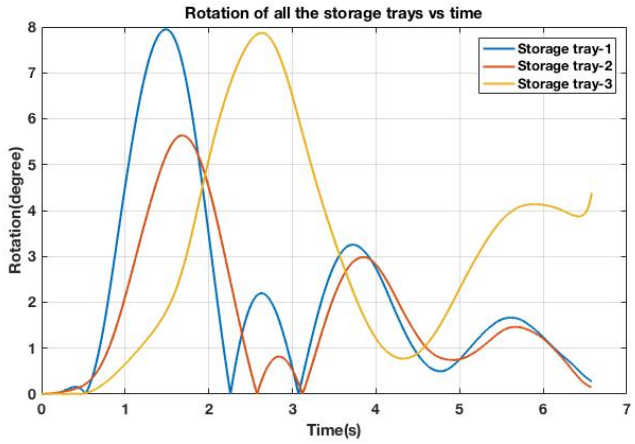

Figure 49: Rotational Tendency with time for spacing of $0.5m$

The rotational tendency of second storage tray is relatively less compared to first and third as observed from the graph. This is probably because of the relative movement of outer storage trays reduce the impact of force of water on the second storage in turn reducing the rotational tendency. The quantification of this phenomenon is shown in the graph. Another result deduced from the contour plot is the increase in the relative spacing between the blocks as they accelerate down the domain.

In addition to that, a comparison is also made between the rotational tendencies of storage trays for single storage and three storage tray cases as shown,

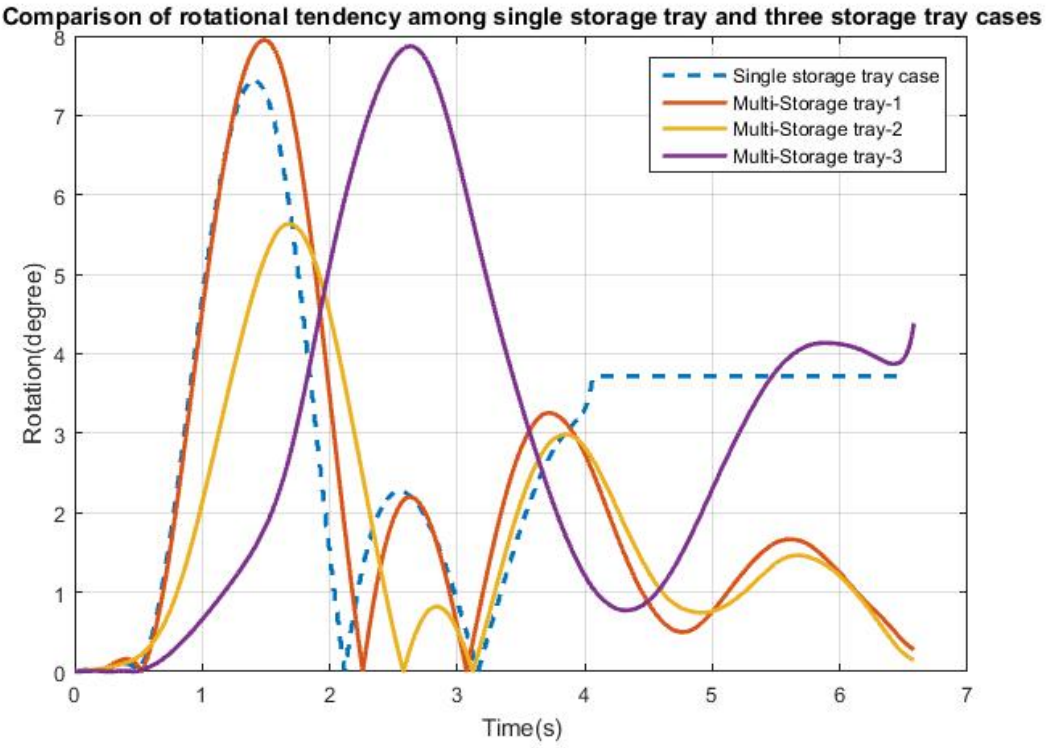

Figure 50: Comparison of rotational tendency for single storage and three storage trays case

The rotational tendency of the last (third) storage tray is relatively dampened as represented by the purple line at the final stages with the time range of $4.5s - 6s$ due to the addition of new storage trays. The distribution of momentum of water among the storage trays reduced the rotating tendency of forces exerted by water on the storage trays. However, in the initial stages of motion, the rotation of first solid storage tray is similar to the single solid storage tray case.

The graph below quantifies the above observation,

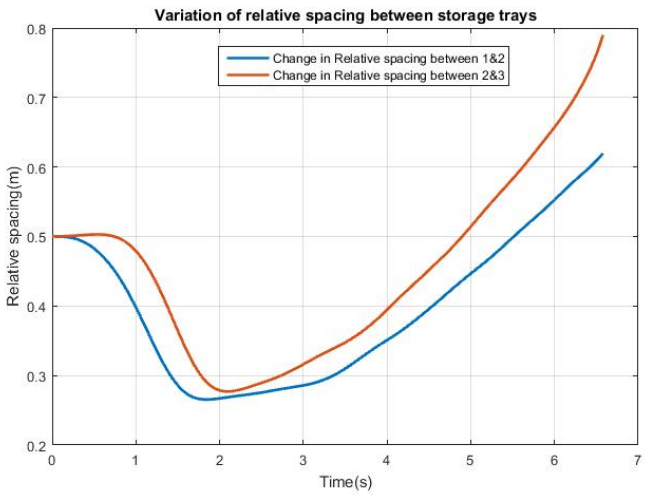

Figure 51: Plot of change in relative spacing with time

From the graphs, in the initial stages, due to domination of vertical forces over horizontal forces leading to vertical oscillations, a reduction in relative spacing is observed. However, as the stability in terms of vertical oscillations is attained, the relative spacing was increasing with time as the velocity in system is yet to reach its steady value.

The rate of increase in spacing was observed to be directly proportional to the initial spacing between the storage trays. The graph below quantifies the above observation,

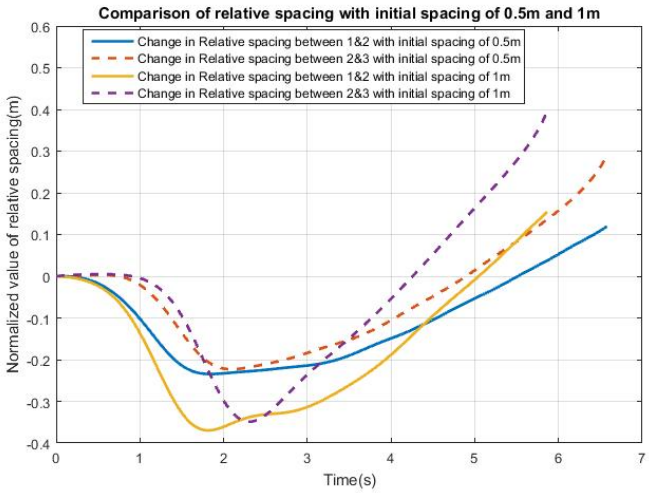

Figure 52: variation of change in relative spacing with initial spacing

The relative spacing between the second and third storage trays was observed to be more influenced by the initial spacing than the first and second storage trays. This is the due to the increase in proximity of the last storage tray to the outlet with increase in initial spacing resulting in higher initial acceleration.

2.4.4 Stability of 4 storage trays with spacing as varying parameter

2.4.4.1 Introduction

From the previous section the minimum required spacing of $0.5m$ is employed for the numerical simulation of 4 storage trays. The objective of this study is to extend the 3 storage stable setup to the four storage case and observe the impact of increased number of storage trays on relative change of spacing.

2.4.5 Geometrical Setup

The domain in this analysis is also increased to $10m$ to sufficiently monitor the motion of all the storage trays. All the other conditions are maintained similar to the single storage tray case.

The geometrical setup of the 4 storage trays is shown below,

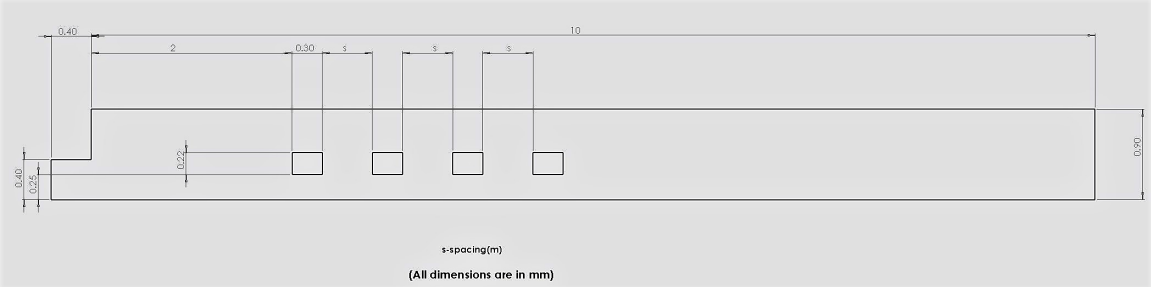

Figure 53: Geometrical setup of the system with 4 storage blocks

The contour plots of density of mixture as a function of initial spacing are shown at specific time values as explained,

1. t = $0s$ - Initial stages of the motion
2. t = $1.5s$ - Intermediate stage where the water tends to slope down due to gravity
3. t = $3.5s$ - Final stages of the motion where the water level is lower.
4. t = $6.009s$ - Final time value where the outermost storage tray reaches the outlet.

The time values above are chosen based on the storage tray's higher rotational and vertical oscillatory behavior.

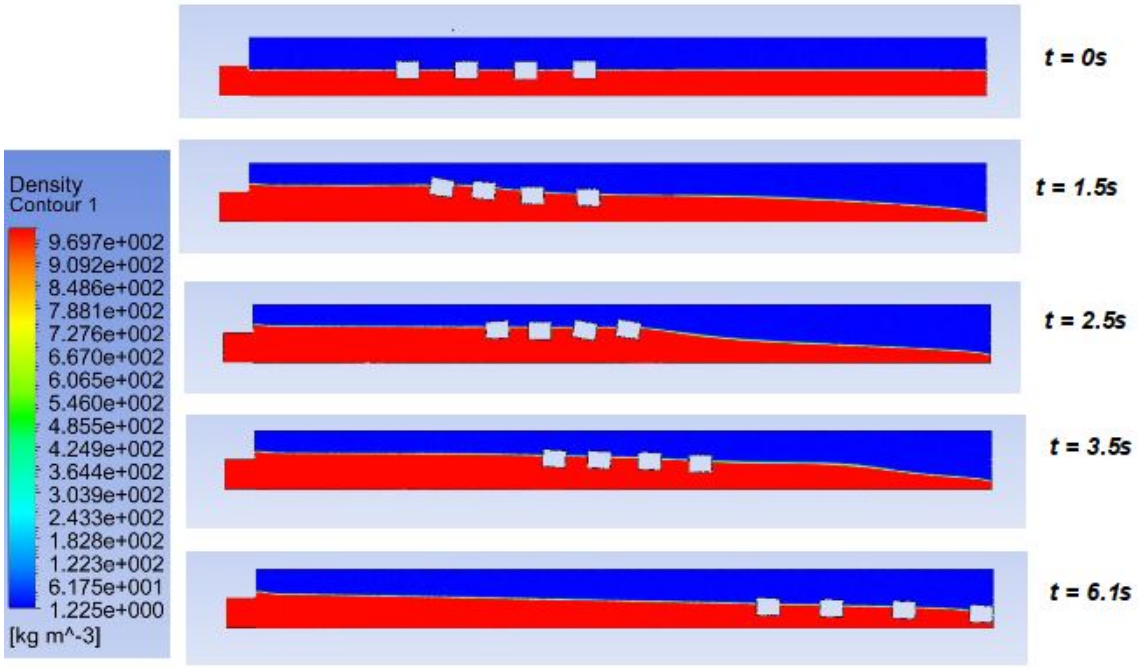

Figure 54: Contour plot of density of mixture for four storage trays with initial spacing of $0.5m$

2.4.5.1 Results and Discussion

From the contour plots, the spacing of $0.5m$ led to a numerically stable solution for addition of the forth storage tray.

The quantification of rotations of storage trays shown in the contours are graphed below,

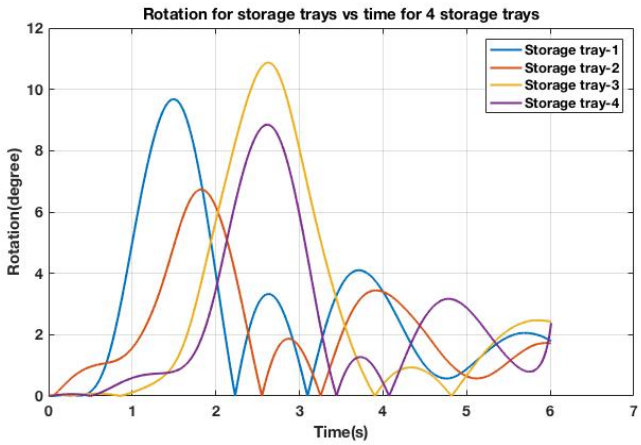

Figure 55: Contour plot of density of mixture for four storage trays with spacing of $0.5m$ at $t = 6.009s$

The rotational tendencies are slightly higher in comparison to the three storage trays case during the initial period. This is expected due to increase in distribution of the momentum of water leading to reduction in driving force and inertial effects of the solid storage trays compared to 3 storage tray case.

In addition to that, a comparison is also made between the rotational tendencies of storage trays for single storage and four storage tray cases as shown,

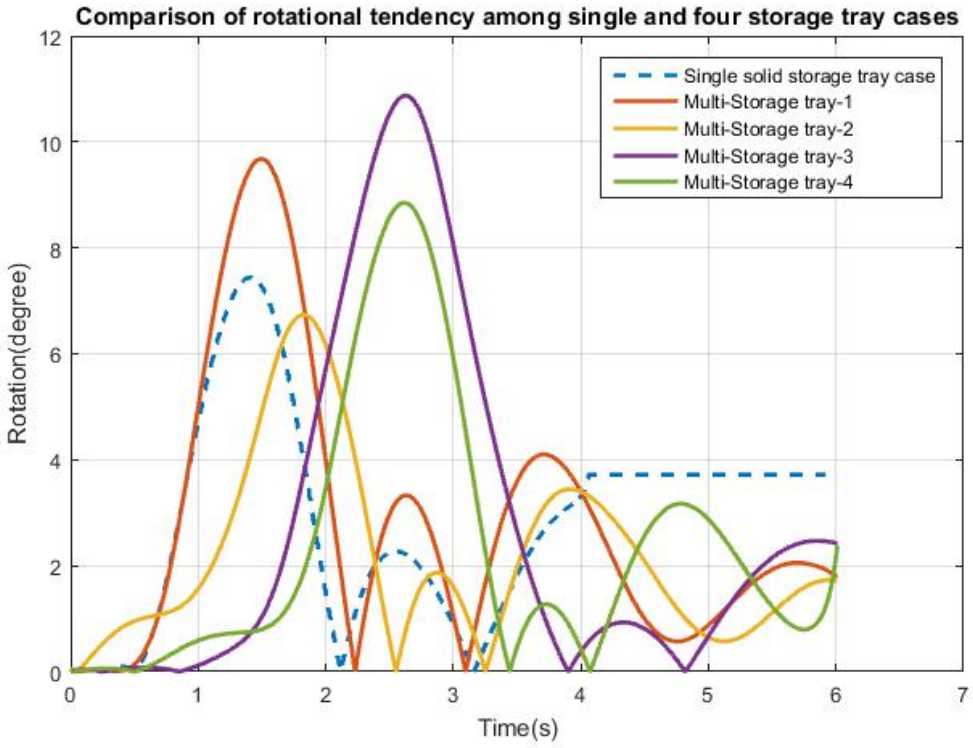

Figure 56: Comparison of rotational tendency for single storage and four storage trays case

The rotational tendency of the storage tray 2 is lesser compared to others which is similar to the three storage trays case. However, the same is not seen for the storage tray 3 due to two reasons:

1. High acceleration of storage tray 4 due to higher proximity to the outlet
2. The position of storage tray 3 is at the point where the water is abruptly sloping down initially.

Another parameter of interest is the spacing. The relative change in spacing between the storage trays is graphed below,

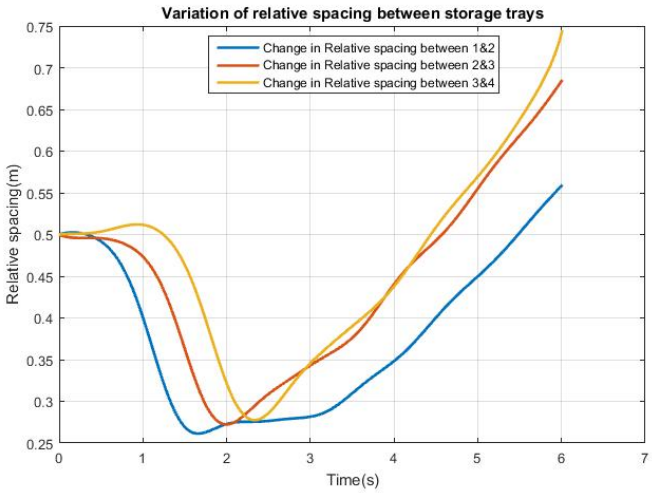

Figure 57: Plot of change in relative spacing with time

From the graphs, similar to the 3 storage tray case, in the initial stages, there is a reduction in relative spacing. However, as the stability in terms of vertical oscillations was attained, the relative spacing was increasing with time.

The increase in spacing for the fourth and third storage tray is higher in comparison to the second and third and second and first. This was expected as the flow was accelerating in nature.

A comparison in terms of change in relative spacing between the three and four storage trays cases is graphed below,

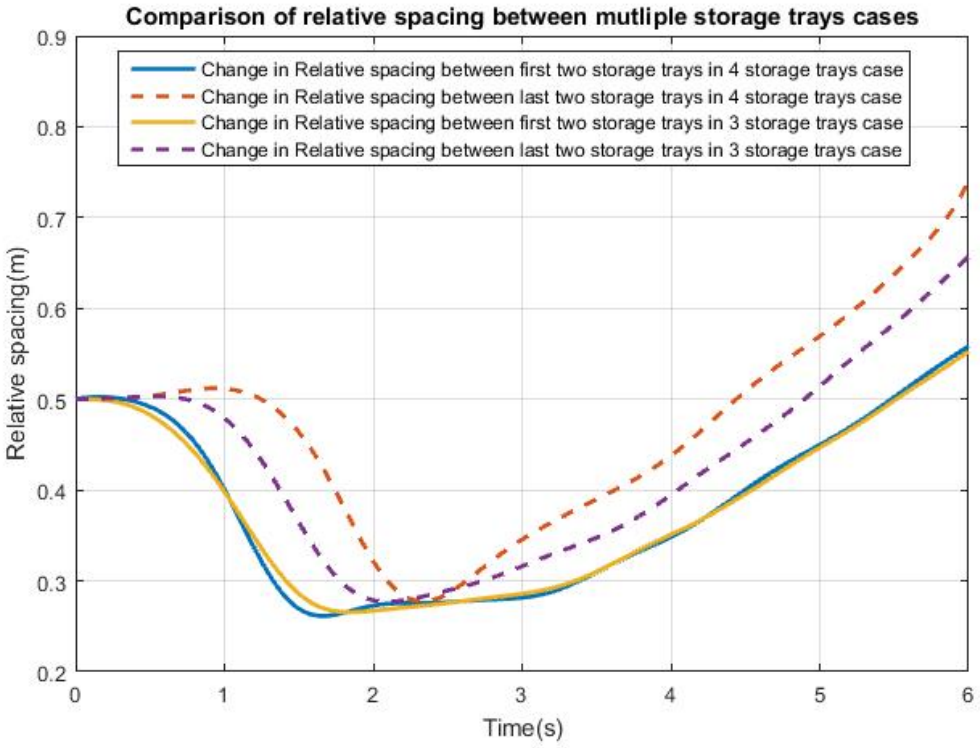

Figure 58: Comparison of rotational tendency of multiple storage tray cases

Chapter 3

CONCLUSION

The study successfully established the solver to perform the numerical simulations for the specified case. The numerical instabilities arising from the combination of the multi phase flow and dynamic mesh are studied and the reasons are summarized below:

1. The numerical instability occurring from the momentary imbalance of the forces due to lower levels of water and lower density of storage tray.
2. The collapse of dynamic mesh discretization due to very low space between the storage trays in the multi storage tray cases.

The study also presented the conditions under which the numerical simulations are numerically stable and represent a virtual experiment. The general range of operating conditions for solid storage tray that are presented in the study are:

Table 1: Prescribed operating conditions for the solid storage tray

Operating Conditions	**Solid**
Density(kg/m^3)	$850 > \rho > 600$
Initial velocity of water(m/s)	$v > 0.7$
Initial depth of water(m)	$0.45 > h > 0.28$

The theory of the optimum conditions of the solid storage tray was successfully extended to the multiple storage trays cases with a minimum required spacing of $0.5m$. In addition, change in relative spacing was observed due to accelerating nature of the flow. This change in relative spacing is shown to increase with increase in initial spacing and addition of storage trays.

Chapter 4

FUTURE WORK

The numerical simulation fails to operate outside the prescribed operating conditions due to numerical instability. So, a recommendation is made to study a more sophisticated solver or a different dynamic mesh setting to incorporate cases outside the operating range.

A study of the motion of the non-uniform and multiple storage trays with varying initial velocity and depth of water is recommended. The relative spacing was increasing with time for multiple storage trays. So, imposing a combination of various non-uniform initial spacing cases for the storage trays and a longer domain is recommended to observe the motion of the storage trays with a steady flow.

An alternative way of depicting a storage tray with non-uniform density is by artificial shifting the center of mass while assigning the values in the dynamic mesh setup. An example of this is shown in the appendix. Utilizing this technique to represent a storage tray with non-uniform density scenario is recommended as a part of future work.

3-D numerical simulations that posses the potential to provide more sophisticated results and help in establishing a refined relation between the motion of the storage tray and the flow are recommended.

REFERENCES

Allshouse, Michael R, Michael F Barad, and Thomas Peacock. 2010. "Propulsion generated by diffusion-driven flow." *Nature Physics* 6 (7): 516.

Bogner, Simon. n.d. "FRIEDRICH-ALEXANDER-UNIVERSITÄT ERLANGEN-NURNBERG."

Bogner, Simon, and Ulrich RüDe. 2013. "Simulation of floating bodies with the lattice Boltzmann method." *Computers & Mathematics with Applications* 65 (6): 901–913.

Fekken, Geert. 2004. "Numerical simulation of free-surface flow with moving rigid bodies."

Gaskell, PH, PK Jimack, M Sellier, HM Thompson, and MCT Wilson. 2004. "Gravity-driven flow of continuous thin liquid films on non-porous substrates with topography." *Journal of Fluid Mechanics* 509:253–280.

Vreugdenhil, Cornelis Boudewijn. 2013. *Numerical methods for shallow-water flow.* Vol. 13. Springer Science & Business Media.

Wörner, Martin. 2012. "Numerical modeling of multiphase flows in microfluidics and micro process engineering: a review of methods and applications." *Microfluidics and nanofluidics* 12 (6): 841–886.

Dynamic Mesh Update Methods. 2009, January. http://www.afs.enea.it/project/neptunius/docs/fluent/html/ug/node396.htm.

Zeng, K, Deepankar Pal, HJ Gong, Nachiket Patil, and Brent Stucker. 2015. "Comparison of 3DSIM thermal modelling of selective laser melting using new dynamic meshing method to ANSYS." *Materials Science and Technology* 31 (8): 945–956.

APPENDIX A

DYNAMIC MESH IN ANSYS FLUENT

A.1 Dynamic Mesh setup in ANSYS Fluent

The following series of images illustrate the steps in setting up dynamic mesh.

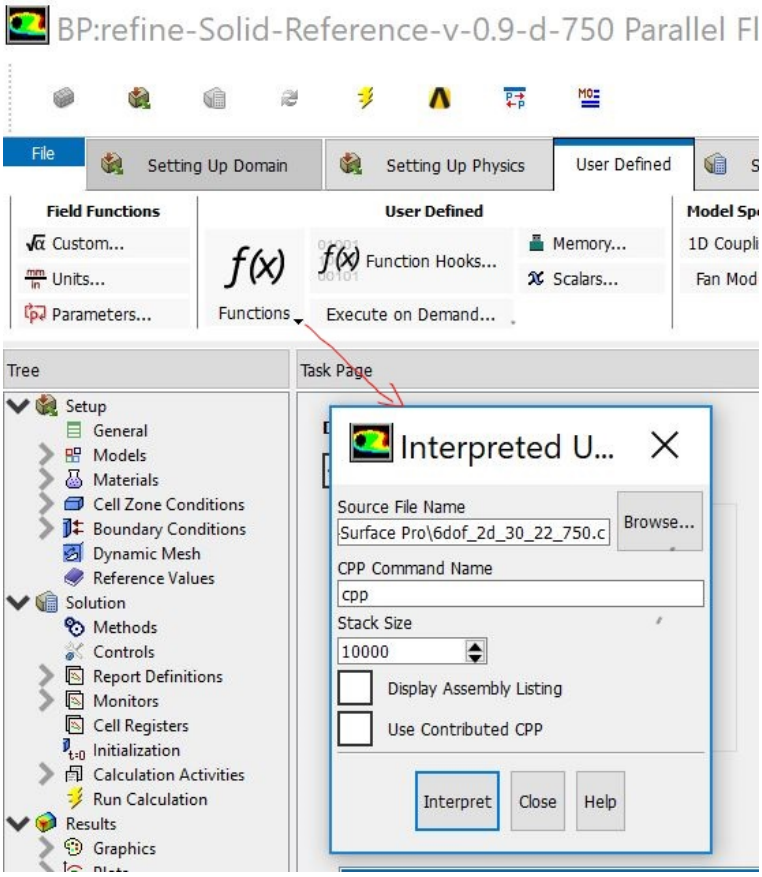

Figure 59: Step-1

The user-defined section enables user to upload a UDF. The UDF can either be compiled or interpreted. In general, ANSYS fluent has a built in interpreter and that makes it an easier option. However for complex codes and high functionality, compiler option is recommended. The compiler option requires ANSYS fluent to be launched from a compiler of Visual Studio.

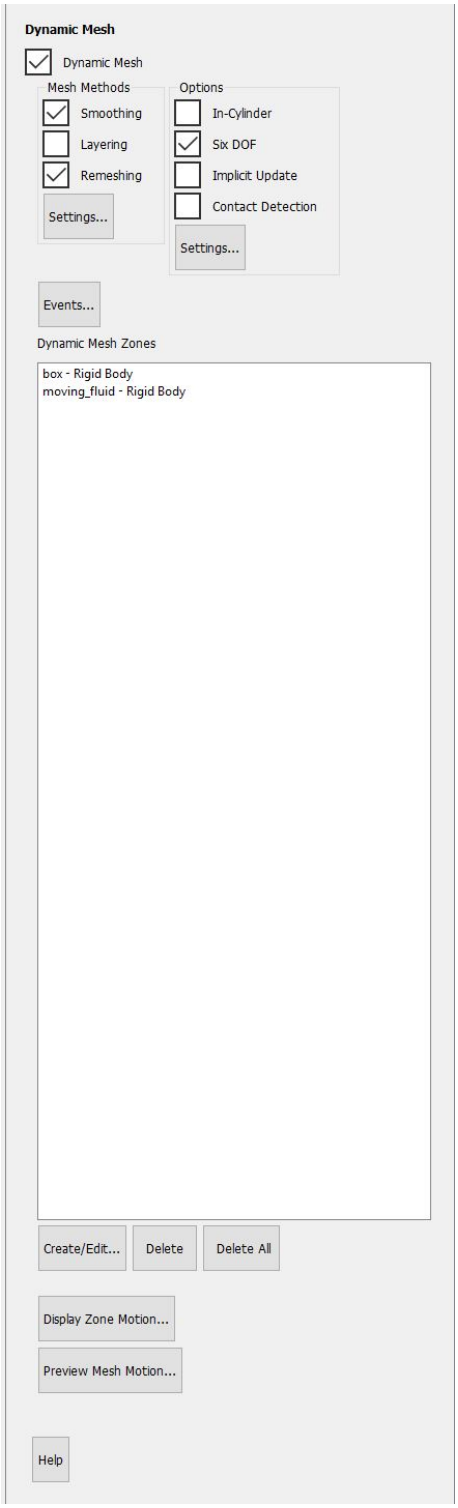

Figure 60: Step-2

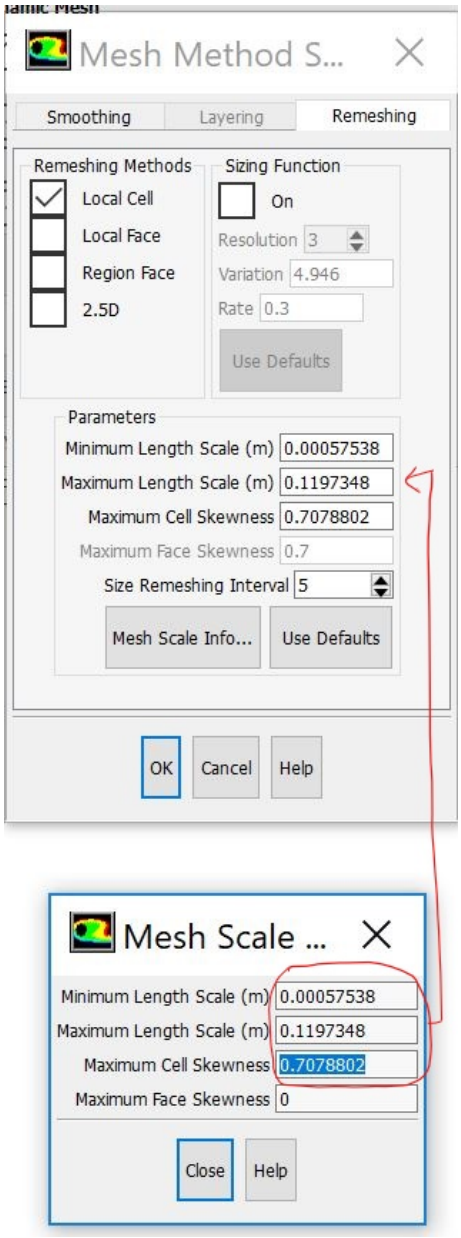

Figure 61: Step-3

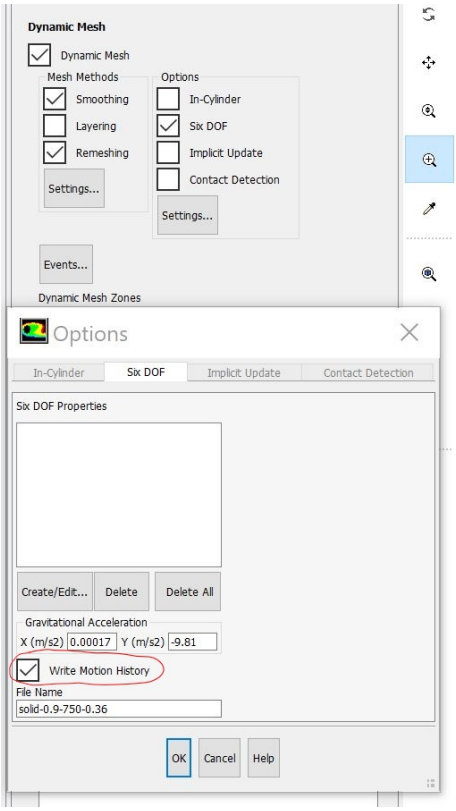

Figure 62: Step-4

The write motion history enables to track the rotation and position of the storage tray with every time step. The data obtained from this file was used to plot the rotational tendency in single storage tray case and rotational tendency and spacing for multi storage trays case using MATALB.

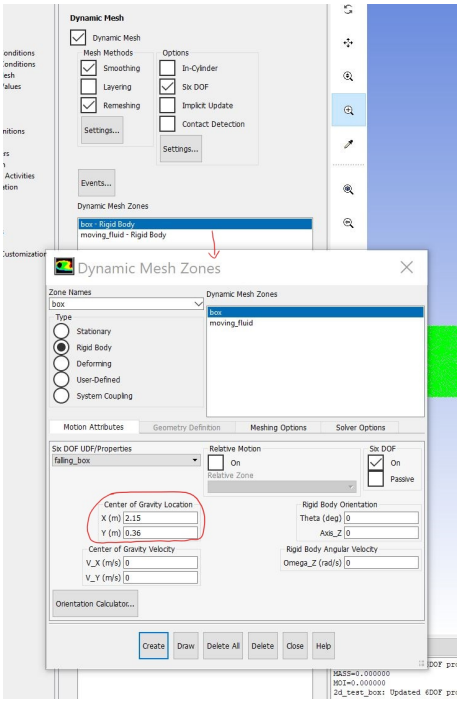

Figure 63: Step-5

The highlighted section of the image is used to enter the center of gravity information. This section also enables users to provide an initial angular rotation and velocity and linear velocity.

A.2 User-defined section(UDF) used in the setting up of dynamic mesh

The user defined function is used to assign properties to the fluid, the object and the moving mesh in the analysis.

```
#include "udf.h"

#define BMODULUS 2.2e9
#define rho_ref 1000.0

------------------Assigning property of fluid in the moving mesh region-----------------------------------------------

DEFINE_PROPERTY(water_density,c,t)
{
    real rho;
    real p, dp, p_operating;

    p_operating = RP_Get_Real("operating-pressure");
    p = C_P(c,t);
    dp = p-p_operating;
    rho = rho_ref/(1.0-dp/BMODULUS);

    return rho;
}

DEFINE_PROPERTY(water_speed_of_sound,c,t)
{
    real a;
    real p, dp, p_operating;

    p_operating = RP_Get_Real ("operating-pressure");
    p = C_P(c,t);
    dp = p-p_operating;
    a = (1.-dp/BMODULUS)*sqrt(BMODULUS/rho_ref);

    return a;
}

---------------Assigning the Mass and Moment of inertia to the solid storage tray and the moving fluid------------

DEFINE_SDOF_PROPERTIES(falling_box_1, prop, dt, time, dtime)
{
   prop[SDOF_MASS] = 46.21;
   prop[SDOF_IZZ] = 0.5329;
   printf ("\n2d_test_box: Updated 6DOF properties");
}
```

Figure 64: UDF for a single storage tray case

For multi storage trays case, the properties of the storage tray need to duplicated with different names as shown. This will help in recognizing and assigning the code in the fluent setup.

```
---------------Assigning the Mass and Moment of inertia to the first solid storage tray and the moving fluid---------------------

DEFINE_SDOF_PROPERTIES(falling_box_1, prop, dt, time, dtime)
{
   prop[SDOF_MASS] = 46.21;
   prop[SDOF_IZZ] = 0.5329;
   printf ("\n2d_test_box: Updated 6DOF properties");
}

---------------Assigning the Mass and Moment of inertia to the second solid storage tray and the moving fluid--------------------

DEFINE_SDOF_PROPERTIES(falling_box_1, prop, dt, time, dtime)
{
   prop[SDOF_MASS] = 46.21;
   prop[SDOF_IZZ] = 0.5329;
   printf ("\n2d_test_box: Updated 6DOF properties");
}
```

Figure 65: UDF for a multi storage tray case

A.3 Moment of inertia information using the "Mass Evaluation Section" in SOLIDWORKS

The non-uniform storage tray cases were designed in SOLIDWORKS software with a depth of $1m$. A custom material was assigned to the design with desired properties. The "Mass Evaluation Section" in the software provides mass moment of inertia information along with position of center of gravity. This feature was verified with the solid storage tray case before implementing in the non-uniform storage tray case.

The details are presented below,

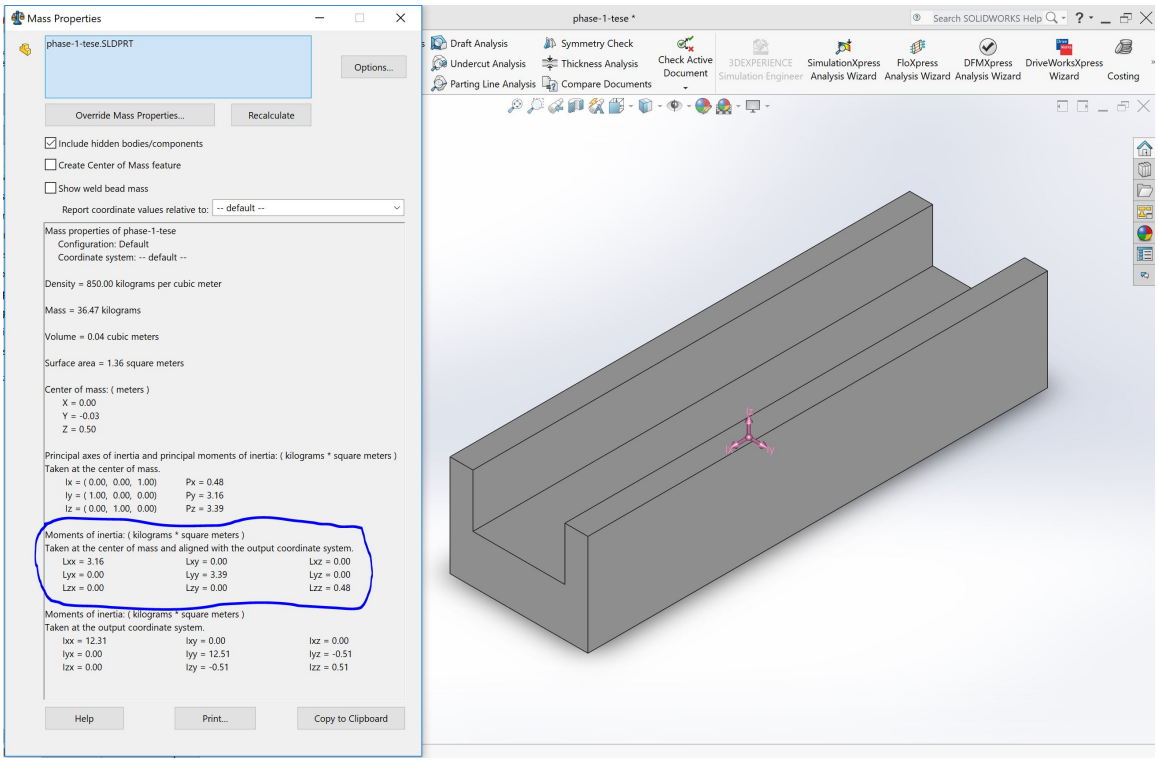

Figure 66: Moment of inertia details of rectangular shaped non-uniform storage tray

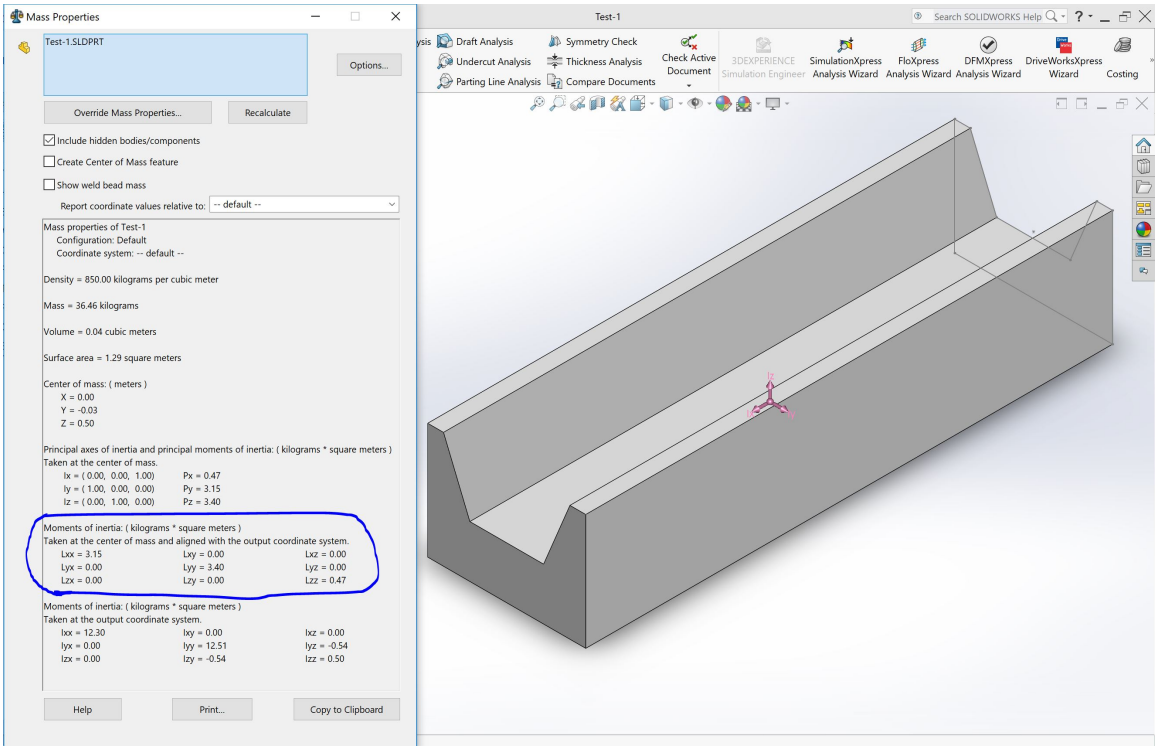

Figure 67: Moment of inertia details of trapezoidal shaped non-uniform storage tray

APPENDIX B

ALTERNATE APPROACH FOR A NON-UNIFORM STORAGE TRAY ANALYSIS

An alternate approach is formulated for the analysis of non-uniform storage trays with $\rho = 850kg/m^3$. This approach eliminates the need for modification of the solid storage design. The required steps for the approach are shown below,

```
DEFINE_SDOF_PROPERTIES(falling_box, prop, dt, time, dtime)
{
   prop[SDOF_MASS] = 44.881;
   prop[SDOF_IZZ] = 0.5201;
   printf ("\n2d_test_box: Updated 6DOF properties");
}
```

Figure 68: User-defined function showing properties of solid storage tray with non-uniform moment of inertia and mass

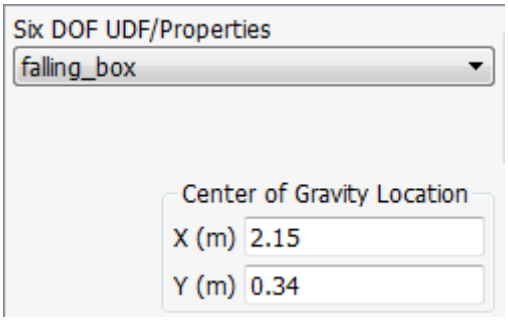

Figure 69: Imposing a shifted center of gravity manually to force non-uniform density scenario

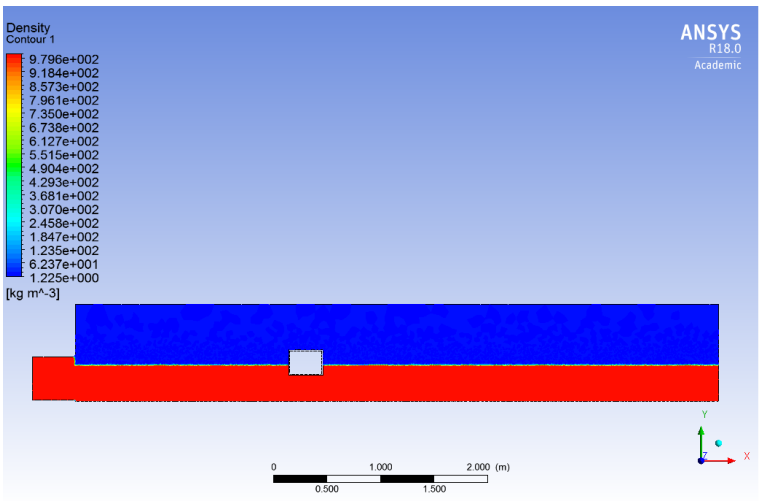

Figure 70: Contour plot of density of mixture at t=0s

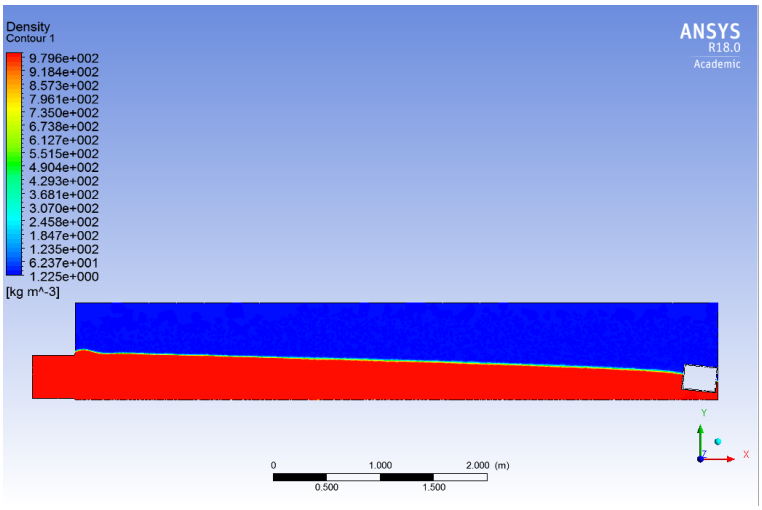

Figure 71: Contour plot of density of mixture at t=t_{final}

APPENDIX C

SURVEY OF EXPERIMENTED CASES

C.1 Boundary Conditions

Various boundary conditions were analyzed before selecting the one used in the report. The summary of the output of various boundary conditions are tabulated below,

Table 2: Survey of different boundary conditions and their implications on the system

Boundary Conditions	**Velocity-inlet(water)**	**Pressure-inlet(water)**
Velocity-inlet(air)	Slow convergence, turbulence in air section	slow convergence
Pressure-inlet(air)	stable solution	sudden drop in water level

C.2 Cases with varying Operating Conditions

Various operating conditions were analyzed before selecting the one used in the report. The summary of the output of various operating conditions are tabulated below,

1. Angle of inclination of domain
    a) High turbulence and numerical instability for $\theta >= 0.01°$. In addition, the storage tray was forced to traverse very fast and its interaction with the gravity driven flow could not be well established.
    b) The angle of inclination of $\theta = 0.001°$ was opted.
2. Length of domain
    a) Lower lengths of $L <= 6m$ fail to provide sufficient time for the development

of flow and subsequent interaction of the storage tray with moving water and air.

b) Higher lengths of $L >= 10m$ are computationally time consuming.

c) Lengths in the range of $6m - 10m$ were opted.

3. Initial velocity of water

a) For very high velocity values of $v >= 1m/s$, the initial flow was very turbulent leading to irregular results and shock formation in the domain.

b) For very low velocity values of $v <= 0.5m/s$, the momentum of water was incapable of driving the storage tray. These cases led to high vertical oscillations and failure of numerical simulation in the initial stages.

c) Velocity values in the range of $0.5m/s$ to $1m/s$ were opted.